Capillary electrophoresis mass spectrometry-based untargeted metabolomics to approach disease diagnosis

Maricruz Mamani-Huanca [a, 1], Alma Villaseñor [a, b, 1], Carolina Gonzalez-Riano [a],
Ángeles López-López [a], Ángeles López-Gonzálvez [a], Coral Barbas [a, *]

[a] Centre for Metabolomics and Bioanalysis (CEMBIO), Department of Chemistry and Biochemistry, Facultad de Farmacia, Universidad San Pablo-CEU, CEU Universities, Urbanización Montepríncipe, 28660, Boadilla del Monte, Madrid, Spain
[b] Departamento de Ciencias Médicas Básicas, Instituto de Medicina Molecular Aplicada (IMMA) Nemesio Díez, Facultad de Medicina, Universidad San Pablo-CEU, CEU Universities, Boadilla del Monte, Spain

ABSTRACT

Metabolites are the final products of the metabolism and are, therefore, directly related to phenotype. They constitute the metabolome of an organism. The wide diversity of the physicochemical properties of the metabolites in terms of molecular weight, concentration, polarity, volatility, solubility, pKa, and charge makes their analysis a remarkable challenge. With over 220,000 metabolites recorded in the HMDB database, there is no single analytical technique capable of analyzing all of them. Therefore, multiple analytical platforms are required to obtain a comprehensive picture of the metabolome. Among these platforms, mass spectrometry (MS)-based analytical techniques are among the most widely used. Capillary electrophoresis (CE) coupled to MS has been employed to analyze polar/ionic metabolites. Although this technique is not widely used, it has demonstrated unique capabilities for the detection of polar and ionic metabolites that are an essential part of the metabolome and are not usually detected by other techniques. This review highlights the role of CE-MS in untargeted metabolomics, particularly in comparison to the hydrophilic interaction chromatography (HILIC) separation mode. Additionally, we discuss the metabolomics workflow in CE-MS for untargeted metabolomics, including sample treatment and analysis, data treatment, and metabolite annotation. We notably present the annotation tools developed explicitly for CE-MS, as well as some computational alternatives, in-house libraries of relative migration times, effective mobility, MS/MS fragmentation, in-source fragmentation, and the CEU Mass Mediator online tool. Finally, we mention future perspectives of this technique, such as single cell-CE and ion mobility (IM)-MS. Overall, this review shows the important role of CE-MS in the studies of untargeted analysis published in the last five years to approach human diseases.

© 2023 The Authors. Published by Elsevier B.V. This is an open access article under the CC BY-NC-ND license (http://creativecommons.org/licenses/by-nc-nd/4.0/).

1. Introduction: untargeted metabolomics

Omics sciences represent an outstanding tool to study biological organisms, providing the opportunity to obtain unexpected findings. These "omics" mainly include genomics, transcriptomics, epigenomics, proteomics, and metabolomics, usually focused on analyzing a large amount of data at each biological level. Just as the genome represents a complete set of genes and the proteome is equivalent to a complete set of proteins, the metabolome constitutes the set of all small molecules (<1500 Da) that can be found in an organism. Metabolites are the result of the last step in a succession of events that start with the DNA. Genes (genome) are transcribed into mRNA (transcriptome), which is translated into proteins (proteome), with metabolites being the final cascade product. Any alteration in genes, transcripts, or enzymes directly impacts metabolites. Thus, metabolites indicate the relationship between metabolism and phenotype [1,2].

Metabolomics has evolved into two approaches: targeted metabolomics, which deals with identifying and quantifying a small group of preselected metabolites usually related to defined biochemical pathways; and untargeted metabolomics, which

* Corresponding author.
E-mail addresses: mar.mamani.ce@ceindo.ceu.es (M. Mamani-Huanca), alma.villasenor@ceu.es (A. Villaseñor), carolina.gonzalezriano@ceu.es (C. Gonzalez-Riano), ang.lopez.ce@ceindo.ceu.es (Á. López-López), alopgon@ceu.es (Á. López-Gonzálvez), cbarbas@ceu.es (C. Barbas).
[1] These authors contributed equally.

consists in the determination of the metabolic fingerprint of a biological sample to identify causal biomarkers usually involved in pathological processes, thus working without any a priori hypothesis [3]. The main objective of an untargeted study is to measure the highest possible number of metabolites present in a biological sample in a single analysis and then reveal the metabolic changes produced by a disease or any other condition through advanced statistical analyses [4].These aspects make the untargeted approach a golden tool for understanding the underlying mechanisms in a pathology, especially for its diagnosis.

2. Analytical techniques in untargeted metabolomics; the role of CE-MS

Although untargeted metabolomics provides excellent tools for the biological analysis of diseases, as previously discussed, the broad coverage of metabolites is complex, and multiple analytical platforms are needed to get a complete picture of the metabolome.

During the last decade, nuclear magnetic resonance spectroscopy (NMR) and mass spectrometry (MS) have been the analytical techniques most widely used for metabolomics. This is because both provide structural information about the significant signals that are subsequently annotated as metabolites [5]. Between them, MS, known for its high sensitivity, has become one of the workhorses in metabolomics. MS can work alone as a direct infusion, or work coupled to different separation techniques such as liquid and gas chromatography (LC and GC, respectively), capillary electrophoresis (CE) or even ion mobility as a pre-MS step (IM-MS) allows the separation of isomeric and isobaric compounds, providing information on the three-dimensional properties of a molecule [6]. In the case of LC, it has become the quintessential separation technique due to its versatility as it combines several chromatographic columns and mobile phases for metabolites with different polarities (from polar to non-polar metabolites) [7]. Among the most common LC separation modes, reversed-phase chromatography, hydrophilic interaction chromatography (HILIC), and ion pair chromatography (IPC) have been used to analyze semi-polar to non-polar metabolites, polar metabolites, and charged metabolites, respectively [8]. Regarding IPC, it is not commonly used in untargeted analysis. However, retention of polar metabolites based on the derivatization for amine groups using 6-aminoquinoloyl-N-hydroxysuccinidimyl carbamate and tributylamine as an ion-pairing agent to retain acids has been recently tested for targeted analysis [9].

HILIC is the most commonly used type of chromatographic separation mode for polar metabolites. However, method development in HILIC is complex due to the wide variety of columns, the long time required to re-equilibrate the system, and the incompatibility between the sample solvent after preparation, which includes organic solvents from mobile phases, and the polarity of the analytes. Despite these inconveniences, new methods are being developed to improve the reproducibility of analyses, retention times in particular [8,10]. Comparing HILIC and CE, it is crucial to consider that the initial conditions for the sample analysis are different [11]. Ironically, in the analysis of highly polar metabolites in HILIC, the sample must be dissolved in the initial mobile phases proportion of the method (usually at least 70% organic phase), while in CE, the sample can be dissolved in water. This sample treatment for HILIC can reduce the solubility of the highly polar metabolites or preclude them from being retained in the column resulting in the loss of information [12]. However, some limitations include the fact that CE is less sensitive than HILIC, as the volume injected is in the range of nanoliters, and it also has an increased migration time (MT) shifting compared to RT in HILIC. All in all, CE is a unique technique for analyzing the polar fraction of the metabolome and, thus, a key platform for untargeted analysis.

Unlike chromatographic methods, in which separation is based on the interaction between the stationary and mobile phases, in CE metabolites are separated according to their charge/size ratio in a background electrolyte solution (BGE) by the influence of an electric field [13−15]. This means that CE is a technique naturally suitable for analyzing highly polar/ionizable metabolites with high separation and selectivity efficiency, and it makes it an orthogonal complement to reversed-phase LC. CE is an ideal technique for working with all types of biological matrices, especially when dealing with restricted sample volumes, as it only requires a few nanoliters. Moreover, CE mostly uses water-based solvents, making it an environmentally friendly technology [14]. Recent revisions regarding interphases, different ionization methods and CE modes have been published elsewhere [16,17]. Because of these aspects, this review aims to show the latest improvements in the untargeted analysis workflow for CE-MS, emphasizing metabolite annotation. In addition, we present the most prominent uses and capabilities of this technique from the last five years for untargeted metabolomics studies in the approach for disease diagnosis. Table 1 shows 48 articles published between 2018 and 2022 where CE-MS was used alone or together with other analytical platforms to obtain biomarkers of different diseases. The table shows the biological sample analyzed, the disease, the size of the cohort (number of samples/patients), the conditions of the CE-MS method, the annotation level that was followed according to the compound identification work group of the Metabolomics Society (i.e., ID confidence level) [18,19], and the significant metabolites. Regarding the ID confidence level, L1 requires the direct comparison with a commercial standard analyzed under identical analytical conditions; L2 is a tentative identification of the metabolite based on the similarity of physicochemical properties such as retention time (RT) or migration time (MT), which also requires a comparison of the MS/MS spectrum with a public/commercial spectral library; level 3 is a tentative annotation obtained from the exact mass, isotopic distribution, and the comparison of the metabolite MS/MS spectrum with its chemical class and L4 pertains to unknown signals [19]. Recently, an L0 has been introduced, which requires full 3D structure and stereochemical information [18].

The studies from Table 1 will be mentioned as examples throughout the text.

3. Metabolomics workflow in CE-MS for untargeted analysis

With some differences, CE-MS follows almost the same workflow for untargeted analysis as LC-MS.

3.1. Sample treatment

The first step is sample treatment. Biological matrices such as urine [20−23] or saliva [24−27] require almost no sample treatment but a dilution. Ultrafiltration is typically only needed to remove proteins in some water-rich samples, such as plasma [28−37], or serum [38−49]. Other strategies, involving organic solvents and water mixtures (e.g. for tissue homogenates), include evaporation to dryness and re-constitution in water before the analysis with CE-MS [50−53]. Regarding cells, metabolite content is obtained after cell disruption by mechanical means such as a homogenizer, or non-mechanical means such as freezing and thawing cycles [54−63] (Fig. 1A).

3.2. Sample analysis

Traditionally, different methods of separation in CE have been reported; however, when coupled to MS for metabolomics,

Table 1
Untargeted and semi-targeted metabolomics studies to approach disease diagnosis using CE-MS.

No	Sample type (Year)	Disease	Sample size	CE conditions	MS conditions	Confidence level and ID	Significant metabolites (&)	Ref.
1	Human plasma (2022)	SARS-CoV-2	N = 57 (27 COVID-19 positive + 30 COVID-19 negative)	Capillary: Fused silica, Voltage: +30 kV. Pressure: 25 mbar. BGE: 1 M FA + 10% (v/v) MeOH. IS: Methionine sulfone	**ESI(+)-TOF**. SL: 50% (v/v) MeOH −H_2O + reference masses	(L2) - m/z + ISF + RMT compared to in-house library	N_2-methyllysine, histidine, tryptophan, glycine, proline, aspartic acid, citrulline, alanine, serine, creatine, 3-aminoisobutyric acid, 2-aminoisobutyric acid, ADMA, SDMA dimethylglycine, phenylalanine, kynurenine, cystine and N-acetylneuraminic acid.	[28]
2	Human plasma (2021)	Parkinson disease (PD)	N = 78 (39 pre-PD + 39 controls)	Capillary: Fused silica. Voltage: +30 kV. Pressure: 25 mbar. BGE: 1 M FA + 10% (v/v) MeOH. IS: Methionine sulfone	**ESI(+)-TOF**. SL: 50% (v/v) MeOH −H_2O + reference masses	(L2) - m/z + ISF + RMT compared to in-house library	2-aminobenzoic acid, 3-methoxytyrosine, pipecolic acid, serotonin and deoxyuridine monophosphate.	[29]
3	Human plasma (2021)	Advanced Neuroendocrine Tumors (NETs)	N = 145 (77 patients with NETs + 68 controls)	Capillary: Fused silica. Pressure: 25 mbar. Voltage: +30 kV. BGE: 1 M FA & 10% (v/v) MeOH. IS: Methionine sulfone	**ESI(+)-TOF**. SL: 50% (v/v) MeOH −H_2O + reference masses	(L2) - m/z + ISF + RMT (L3) - m/z	(&) - (↑) arginine, Arg-Val, SDMA, galactosyl-hydroxy-lysine, gamma-glutamyl-ornithine, Glu-Ala, Glu-Arg, Glu-hyp, Glu-Lys/ℇ-Glu-Lys, glutamine, homocitrulline, Lys-Asp, methionine S-oxide, N-acetyl-lysine, pyroglutamine, Ser-hyp, Thr-Ala, Val-Leu, acetylspermidine, glucosylgalactosylhydroxylysine, methylimidazole, nicotinamide N-oxide/ urocanate, 1-methyladenosine, norcotinine, piperideine, serotonine, hypoxanthine, 8-hydroxycarteolol and 5,6-dihydrothymine. (↓) aspartate, Cys-Gly, Cys-Gly disulfide, cysteineglutathione disulfide, Gly-Pro, iminodiacetic acid, N_2-methyl-lysine, N_2-methylproline, N_6-acetyl-hydroxylysine, ornithine, phenylalanine, Ser-Ala, Ser-Val, Thr-Gly, 1-aminocyclohexanecarboxylic acid, 9-decenoylcarnitine, 8-hydroxycarteolol.	[30]
4	Human plasma (2021)	Metabolic syndrome (MetS) in early childhood	N = 456 (228 cases of MetS + 228 controls)	**MSI-CE**. Capillary: Fused silica. Voltage: +30 kV. BGE: 1 M FA with 15% ACN (pH 1.8). IS: 3-chloro-L-tyrosine + $^{13}C_6$-glucose. Capillary: Fused silica. Voltage: +30 kV. Pressure: 2 mbar/min (pressure gradient). BGE:50 mM NH_4HCO_3 (pH 8.5). IS: 3-chloro-L-tyrosine and $^{13}C_6$-glucose	**ESI(+)-TOF**. SL: 60% (v/v) MeOH −H_2O with 0.1% FA + reference masses **ESI(−)-TOF**. SL: 50% (v/v) MeOH −H_2O + reference masses	(L1) - mass accuracy + RMT compared to in-house database + confirmed by standards	(↑) glucose, alanine, threonine, carnitine, tyrosine, and monomethylarginine. (↓) tryptophan and glutamine/glutamate.	[31]
5	Human plasma (2021)	Fontan procedure in children with univentricular hearts	N = 31 (14 patients after the Fontan procedure + 17 controls: 8 healthy and 9 patients after biventricular repair)	Capillary: Fused silica. Voltage: +30 kV. BGE: 1 M FA. IS: Methionine sulfone + D-camphor-10-sulfonic acid. Capillary: SMILE(+). Voltage: −30 kV. BGE: 50 mM NH_4Ac (pH 8.5). IS: Methionine sulfone + D-camphor-10-sulfonic acid	**ESI(+)-TOF**. SL: 50% (v/v) MeOH −H_2O + reference masses **ESI(−)-TOF**. SL: 5 mM NH_4Ac in 50% (v/v) MeOH −H_2O + reference masses	(L1) -m/z + MT compared to HMT metabolite database + confirmed by standards	(‡) (↑) hypoxanthine, methionine, phenylalanine, tryptophan (↓) arginine, tyrosine and citrulline (increase in Biventricular group). (↑) 2-oxoglutaric acid, cis-aconitic acid, gluconic acid, isocitric acid, lactic acid, malic acid.	[32]
6	Human plasma (2020)	Very preterm infants (VPI) with extrauterine growth restricted (EUGR)	N = 51 (29 corresponded to preterm babies with weight at discharge over the 10th percentile for postmenstrual age + 22 to EUGR patients)	Capillary: Fused silica. Voltage: +30 kV. Pressure: 25 mbar. BGE: 1 M FA. IS: Methionine sulfone	**ESI(+)-TOF**. SL: 50% (v/v) MeOH −H_2O + reference masses	(L1) - m/z + RMT compared to in-house library + confirmed by standards	(&) - Markers related to amino acid metabolism, particularly branched-chain amino acids, and changes in lipid species.	[33]

Table 1 (*continued*)

No	Sample type (Year)	Disease	Sample size	CE conditions	MS conditions	Confidence level and ID	Significant metabolites (&)	Ref.
7	Human plasma (2018)	Ossification of the posterior longitudinal ligament (OPLL)	$N = 20$ (10 patients with cervical OPLL + 10 control subjects)	Capillary: Fused silica. Voltage: +30 kV. BGE: 1 M FA. IS: not available	**ESI(+)-TOF**. SL: NH$_4$Ac (5 mM) in 50% (v/v) MeOH $-$H$_2$O	(L2) - m/z + MT compared to HMT library	(&,‡) - (↑) Acylcarnitine (14:0), palmitoylcarnitine (18:2), fatty acid (24:2), thyroxine, thiaproline in OPLL group.	[34]
				Capillary: SMILE(+). Voltage: $-$30 kV. BGE: 50 mM NH$_4$Ac (pH 8.5). IS: not available	**ESI($-$)-TOF**. SL: NH$_4$Ac (5 mM) in 50% (v/v) MeOH $-$H$_2$O			
8	Human plasma (2018)	Cachexia	$N = 15$ (8 cachectic + 7 non-cachectic patients)	Capillary: Fused silica. Voltage: +30 kV. Pressure: 25 mbar. BGE: 1 M FA. IS: Methionine sulfone	**ESI(+)-TOF**. SL: 50% (v/v) MeOH $-$H$_2$O + reference masseso	(L1) - m/z + RMT compared to in-house library	(&) - (↓) arginine, tryptophan, indolelactic acid, threonine, lysophosphatidylcholines(O-16:0), lysophosphatidylcholines(20:3), and sphingolipids.	[35]
9	Human plasma & urine (2019)	Phenylketonuria (PKU): assessment of dietary adherence & nutritional deficiencies	$N = 22$ PKU phenotype, including patients with poor diet control (plasma Phe >360 μM, n = 9) as compared to optimal diet adherence (plasma Phe <360 μM, n = 7)	MSI-CE. Capillary: Fused silica. Voltage: +30 kV. BGE: 1 M FA and 15% (v/v) ACN at pH 1.8. IS: 3-chlorotyrosine, + naphthalene monosulfonic acid. Capillary: COSMO(+). Voltage: $-$30 kV. BGE: 50 mM NH$_4$Ac (pH 8.5). IS: not available	**ESI(+)-QTOF**. SL: 60% (v/v) MeOH with 0.1% FA + reference masses **ESI($-$)-QTOF**. SL: NH$_4$Ac (5 mM) in 50% (v/v) MeOH $-$H$_2$O + reference masses	(L2) - m/z + RMT + tandem MS/MS	(↓) concentrations of tyrosine, arginine, 2-aminobutyric acid, and propionylcarnitine in plasma that were inversely correlated to phenylalanine in non-adherent PKU patients. (↑) concentrations of catabolites indicative of phenylalanine intoxication (phenylpyruvic acid, phenylacetylglutamine, hydroxyphenylacetic acid) in the urine associated with poor dietary adherence among PKU patients. PKU patients with poor blood phenylalanine control had (↓) excretion of urinary compounds derived from co-metabolism of tyrosine (cresol sulfate, phenylsulfate), folic acid, and vitamin B12.	[36]
10	Human plasma & urine (2019)	Rheumatoid arthritis (RA)	$N = 49$ 32 patients with active RA and 17 with inactive RA	Capillary: Fused silica. Voltage: +27 kV. BGE: 1 M FA. IS: H3304-1004, HMT Capillary: Fused silica. Voltage: +30 kV. BGE: 50 mM NH$_4$Ac (pH 8.5). IS: not available	**ESI(+)-TOF**. SL: Commercial (H3301-1020, HMT) **ESI(+)-TOF**. SL: Commercial (H3301-1020, HMT)	(L2) - m/z + MT compared to HMT library	(‡) (↓) histidine and guanidoacetic acid in plasma and (↑) hypotaurine in urine.	[37]
11	Human serum (2022)	Diet biomarkers in pregnancy	$N = 273$ pregnant women in their second trimester	**MSI-NACE**. Capillary: Fused silica. Voltage: +30 kV. Pressure: 20 mbar. BGE: 35 mM NH$_4$Ac in ACN-MeOH $-$H$_2$O$-$IPA (70:15:10:5, v/v/v/v) (pH 9.5). IS: deuterated stearic acid.	**ESI($-$)-TOF**. SL: 80% (v/v) MeOH $-$H$_2$O whit 0.5% (v/v) NH$_4$OH	(L1) - ID + QTF using standards	Odd-chain NEFAs (pentadecanoic and heptadecanoic acids) were associated with intake of full-fat dairy products, as well as with glucose intolerance. Moreover, docosahexaenoic had a correlation to self-reported fish/fish oil intake. On the other hand, decanoic acid was weakly associated with butter intake and myristic acid was associated with intake of full-fat dairy products.	[38]
12	Human serum (2022)	Gestational diabetes mellitus (GDM)	$N = 590$ pregnant women (South Asia: 81 patients with GMD + 218 controls; white European: 52 patients with GMD + 291 controls)	**MSI-CE**. Capillary: Fused silica. Voltage: +30 kV. BGE: 1 M FA with15% vol ACN. IS: 3-chloro-L-tyrosine. **MSI-CE**. Capillary: Fused silica. Voltage: +30 kV. Pressure: 2 mbar/min (pressure gradient). BGE: 50 mM NH$_4$HCO$_3$ (pH 8.5). IS: 3-chloro-L-tyrosine.	**ESI(+)-QTOF**. SL: 50% (v/v) MeOH $-$H$_2$O with 0.1% FA **ESI($-$)-QTOF**. SL: 50% (v/v) MeOH $-$H$_2$O	(L2) - m/z, RMT, tandem MS/MS (L4) - molecular formula, RMT	(↑) glutamic acid, propionylcarnitine, tryptophan, arginine, 2-hydroxybutyric acid, 3-hydroxybutyric acid, pyruvic acid, and 3-methyl-2-oxovaleric acid were associated with higher probabilities of GDM. Additionally (↑) glutamine, ornithine, oxoproline, cystine, and glycine were inversely related to GDM. In addition, (↑) ratios of glucose/glutamine, glucose/creatinine, glutamic acid/glutamine and arginine/ornithine were found to be predictors of GDM.	[39]

13	Human serum (2022)	Nonalcoholic Steatohepatitis (NASH) (Metabolic profiling)	N = 85 NASH patients	**MSI-NACE**. Capillary: Fused silica. Voltage: +30 kV. BGE: 35 mM NH₄Ac in ACN–MeOH–H₂O–IPA (70:15:10:5, v/v/v/v) (pH 9.5). IS: deuterated stearic acid	**ESI(−)-Orbitrap**. SL: 80% (v/v) MeOH −H₂O whit 0.5% (v/v) NH₄OH	(L2) - m/z + RMT + MS/MS using LIPIDMAPS (L3) - m/z, RMT	270 serum lipid features were reported, including phosphatidylcholines, phosphatidylinositols, phosphatidylethanolamines, lysophosphatidic acids, bile acids and prostaglandins	[40]
14	Human serum (2021)	Chronic kidney disease (CKD)	N = 24 (11 hemodialysis patients + 13 Non-hemodialysis with CKD)	Capillary: Fused silica. Voltage: +30 kV. BGE: 1 M FA. IS: Methionine sulfone, MES, 3-aminopyrrolidine and D-camphor-10-sulfonic acid. Capillary: COSMO (+). Voltage: −30 kV. BGE: 50 mM NH₄Ac (pH 8.5). IS: Methionine sulfone, MES and D-camphor-10-sulfonic acid.	**ESI(+)-TOF**. SL: 50% (v/v) MeOH −H₂O + reference masses **ESI(−)-TOF**. SL: NH₄Ac (5 mM) in 50% (v/v) of MeOH −H₂O + reference masses	(L1) - m/z + RMT compared to standards	Metabolites present only in hemodialysis patients (N-acetylneuraminic acid and benzoate). Thirty-eight compounds were found to be (↑) and 23 compounds (↓) compared to non-hemodialysis patients with CKD.	[41]
15	Human serum (2021)	Musculoskeletal diseases (Osteoporosis & sarcopenia)	N = 729 (of which 35 patients developed osteoporosis +39 recently diagnosed with sarcopenia)	Capillary: Fused silica. Voltage: +30 kV. BGE: 1 M FA. IS: Methionine sulfone and D-camphor-10-sulfonic acid. Capillary: COSMO (+). Voltage: −30 kV. BGE: 50 mM NH₄Ac (pH 8.5). IS: Methionine sulfone and D-camphor-10-sulfonic acid.	**ESI(+)-TOF**. SL: 50% (v/v) MeOH −H₂O + reference masses **ESI(−)-TOF**. SL: NH₄Ac (5 mM) in 50% (v/v) of MeOH −H₂O + reference masses	(L1) - m/z + RMT compared to standards	(↑) serum glycine levels predicted the development of new osteoporosis within four years, but not the development of sarcopenia. On the other hand, (↓) serum taurine levels were associated with the new development of sarcopenia but not osteoporosis within four years.	[42]
16	Human serum (2021)	Liver fibrosis in chronic hepatitis C virus (HCV)	N = 34 (20 HVC patients + 14 controls)	**MSI-CE**. Capillary: Fused silica. Voltage: +30 kV. Pressure: 2 mbar/min (pressure gradient). BGE: 1 M FA with15% vol ACN. IS: 4-chlorotyrosine and naphthalene monosulfonic acid. **MSI-CE**. Capillary: Fused silica. Pressure: 2 mbar/min (pressure gradient). Voltage: +30 kV. BGE: 50 mM NH₄HCO₃ (pH 8.5). IS: 4-chlorotyrosine and naphthalene monosulfonic acid.	**ESI(+)-TOF**. SL: 60% (v/v) MeOH −H₂O with 0.1% FA **ESI(−)-TOF**. SL: 50% (v/v) MeOH −H₂O	(L1)- m/z + RMT compared to standards	(↑) choline, histidine, oxo-proline and glutathione were reported in HCV patients.	[43]
17	Human serum (2020)	Peripheral artery disease (PAD)	N = 38 PAD participants clinically stratified into chronic limb-threatening ischemia (CLTI, n = 18) + intermittent claudication (IC, n = 20). Non-PAD controls (n = 20)	**MSI-CE**. Capillary: Fused silica. Voltage: +30 kV. BGE: 1 M FA with 13% vol ACN (pH 1.8). IS: not available. **MSI-CE**. Capillary: Fused silica. Voltage: +30 kV. Pressure: 2 mbar/min (pressure gradient). BGE: 35 mM NH₄Ac (pH 9.5). IS: not available. **MSI–NACE**. Capillary: Fused silica. Voltage: +30 kV. Pressure: 20 mbar. BGE: 35 mM NH₄Ac in ACN–MeOH −H₂O–IPA (70:15:10:5, v/v/v/v) (pH 9.5). IS: not available.	**ESI(+)-TOF**. SL: 60% (v/v) MeOH −H₂O with 0.1% FA + reference masses **ESI(−)-TOF**. SL: 80% (v/v) MeOH −H₂O + reference masses **ESI(−)-TOF**. SL: interface kit: 80% (v/v) MeOH−H₂O whit 0.5% NH₄OH + reference masses	(L1) - m/z + RMT, confirmed with standards (L2) - m/z + RMT (L4) - unknowns by molecular formula	(↓) creatine, histidine, lysine, oxoproline, monomethylarginine, and (↑) phenylacetylglutamine in PAD patients CLTI cases exhibited (↑) of carnitine, creatinine, cystine, trimethylamine-N-oxide, and (↓) fatty acids. The ratio between stearic acid to carnitine, and arginine to propionylcarnitine dierentiated on CLTI from IC.	[44]

Table 1 (continued)

No	Sample type (Year)	Disease	Sample size	CE conditions	MS conditions	Confidence level and ID	Significant metabolites (&)	Ref.
18	Human serum (2019)	Rheumatoid arthritis (RA)	$N = 43$ RA patients were classified to have a good response, moderate, or no response, 12 weeks after starting the biological treatment regimen. 14 of 26 patients in the TNF-a inhibitors (TNFi) group and 6 of 17 patients in the abatacept (ABT) group respondedto the biologic treatment	Capillary: Fused silica. Voltage: +30 kV. BGE: commercial buffer (H3301-1001). IS: not available. Capillary: SMILE(+). Voltage: −30 kV. BGE: commercial buffer (H3302-1021). IS: not available.	**ESI(+)-TOF**. SL: 50% (v/v) MeOH −H₂O + reference masses **ESI(+)-TOF**. SL: NH₄Ac (5 mM) in 50% (v/v) MeOH −H₂O + reference masses	(L2) - m/z + MT compared to HMT library	(‡) Five metabolites (betonicine, glycerol 3-phosphate, N-acetylalanine, hexanoic acid and taurine) as potential predictors of TNFi responders, and three (citric acid, quinic acid, and 3-aminobutyric acid) as predictors of ABT responders.	[45]
19	Human serum (2019)	Future onset of coronary artery disease (CAD) in patients with type 2 diabetes mellitus	$N = 55$ (16 subjects who suffered from a CAD event during the observation period + 39 non-CAD subjects who were matched to the CAD group)	not available	**ESI(+)-TOF**. SL: not available	(L2) - m/z + MT compared to HMT library	(‡) (↓) pelargonic acid, glucosamine: galactosamine, thymine, 3-hydroxybutyric acid, creatine, 2-aminoisobutyric acid, hypoxanthine in the CAD group compared with the non-CAD group.	[46]
20	Human serum (2019)	Overactive bladder (OAB)	$N = 58$ (32 control + 26 OAB)	Capillary: Fused silica. Voltage: +30 kV. BGE: H3301-1001 HMT. IS: H3304-1004, HMT. Capillary: SMILE (+). Voltage: −30 kV. BGE: H3302-1021. IS: not available.	**ESI(+)-TOF**. SL: Commercial (H3301-1020, HMT) **ESI(+)-TOF**. SL: Commercial (H3301-1020, HMT)	(L2) - m/z + MT compared to HMT library	(‡) (↑) glutamate, arginine, glutamine and inosine monophosphate. (↓) asparagine and hydroxyproline.	[47]
21	Human serum (2019)	Nocturia	$N = 66$ (45 with nocturia +21 controls)	Capillary: Fused silica. Voltage: not available. BGE: commercial buffer (H3301-1001). IS: not available. Capillary: Fused silica. Voltage: not available. BGE: commercial buffer (I3302-1023). IS: not available.	**ESI(+)-TOF**. SL: not available **ESI(+)-TOF**. SL: not available	(L2) - m/z + MT compared to HMT library	(‡)(↑) lauric acid and imidazolelactic acid, and (↓) thiaproline and glycerol.	[48]
22	Rat serum (2022)#	Treatment for rejuvenation in aged rats with human placenta-derived mesenchymal stem cells (hPD-MSCs)	$N = 48$ female treated rats (24 treated with hPD-MSC + 24 controls)	Capillary: Fused silica. Voltage: +27 kV. BGE: 1 M FA. IS: not available Capillary: Fused silica. Voltage: +30 kV. BGE: 50 mM NH₄Ac (pH 7.5). IS: MES.	**ESI(−)-Orbitrap**. SL: NH₄Ac (5 mM) in 50% (v/v) of MeOH −H₂O + reference masses **ESI(−)-TOF**. SL: NH₄Ac (5 mM) in 50% (v/v) of MeOH −H₂O + reference masses	(L2) - m/z + MT compared to HMT library	(‡)(↑) 3-hydroxybutyric acid, glycocholic acid, and taurine associated with health and longevity, and increased after stimulation of hPD-MSCs.	[49]
23	Human dried blood spot (2019)	Cystic fibrosis (CF)	$N = 80$ Normal birth weight CF neonates without meconium ileus (n = 36) + gestational age/sex-matched screen-negative controls (n = 44)	MSI-CE Capillary: Fused silica. Voltage: +30 kV. BGE: 1 M FA and 15% (v/v) ACN at pH 1.8. IS: 3-chlorotyrosine, and naphthalene monosulfonic acid.	**ESI(+)-QTOF**. SL: 60% (v/v) MeOH −H₂O with 0.1% FA + reference masses	(L1) - m/z + RMT compared to standards + confirmed by standards Structural elucidation of unknowns by tandem MS/MS	CF-specific biomarker candidates included several amino acids (↓) in circulation (tyrosine, serine, threonine, proline, glycine). Additionally, CF neonates had (↓) ophthalmic acid and (↑) of an unknown trivalent peptide.	[122]

	Sample (year)	Disease	N	CE conditions	MS conditions	Annotation	Main findings	Ref.
24	Human urine (2022)	Colorectal cancers (CRCs)	$N = 284$ (36 healthy controls, 34 adenoma, 214 CRC samples)	Capillary: Fused silica. Voltage: +30 kV. BGE: 1 M FA. IS: Methionine sulfone. Capillary: COSMO (+). Voltage: −30 kV. BGE: 50 mM NH$_4$Ac (pH 8.5). IS: D-camphor-10-sulfonic acid.	**ESI(+)-TOF**. SL: 50% (v/v) MeOH −H$_2$O + reference masses **ESI(−)-TOF**. SL: NH$_4$Ac (5 mM) in 50% (v/v) MeOH −H$_2$O + reference masses	(L2) - m/z + RMT compared to standards	Biomarkers validation. The metabolites, γ-guanidinobutyrate, asparagine, 3-methylhistidine, 1-methyladenosine, 3-hydroxybutyrate, N-acetylglutamate, hippurate, methionine, 7,8-dihydrobiopterin and sebacate, showed the greatest predictive ability.	[20]
25	Human urine (2021)	Acute kidney injury (AKI)	$N = 121$ two groups. Group 1 (14 severe AKI patients, 24 mild AKI patients, 23 controls). Group 2 (20 mild AKI patients, 40 controls)	Capillary: Fused silica. Voltage: +30 kV. BGE: 1 M FA. IS: Methionine sulfone and 3-aminopyrrolidine. Capillary: COSMO (+). Voltage: −30 kV. BGE: 50 mM NH$_4$Ac (pH 8.5). IS: D-camphor-10-sulfonic acid and MES.	**ESI(+)-TOF**. SL: 50% (v/v) MeOH −H$_2$O + reference masses **ESI(−)-TOF**. SL: NH$_4$Ac (5 mM) in 50% (v/v) of MeOH −H$_2$O + reference masses	(L1) - m/z + RMT compared to standards (L4) - m/z + RMT predicted by (ANNs)	512 known metabolites were quantified + identified 155 unknown peaks. Glycine, urea, uric acid, ethanolamine, glutamine, N,N-dimethylglycine were found to be significantly (↓) in subjects with mild or severe AKI compared to those without AKI. Significant metabolites in group 2 (piperidine, taurine, methanesulfonate, 3-hydroxykynurenine).	[21]
26	Human urine (2021)	Inflammatory bowel disease (IBD) in pediatric patients	$N = 26$ (18 Crohn's disease (CD) patients + 8 Ulcerative colitis (UC) patients)	**MSI-CE**. Capillary: Fused silica. Voltage: +30 kV. BGE: 1 M FA with15% vol ACN (pH 1.8). IS: 3-chloro-L-tyrosine and 2-naphthalenesulfonate **MSI-CE**. Capillary: Fused silica. Voltage: +30 kV. Pressure: 2 mbar/min (pressure gradient). BGE: 50 mM NH$_4$HCO$_3$ (pH 8.5). IS: 3-chloro-L-tyrosine and 2-naphthalene-sulfonate	**ESI(+)-QTOF**. SL: 60% (v/v) MeOH −H$_2$O with 0.1% FAo **ESI(−)-QTOF**. SL: 50 mM NH$_4$Ac in 50% (v/v) of MeOH −H$_2$O	(L1) - spiking pooled urine with standards(L2) - m/z + MS/MS spectral comparisons to public databases (L3) - fragment ions and neutral losses	(↑) urinary indoxyl sulfate, hydroxyindoxyl sulfate, phenylacetylglutamine and sialic acid reported in CD patients compared with UC, while (↓) threonine, serine, kynurenine, and hypoxanthine.	[22]
27	Newborn human urine (2021)	Neonatal encephalopathy (NE)	$N = 279$ two groups 33 pathological + 22 controls (35 samples were collected before therapeutic hypothermia (HT), 44, 52, 53, 53 + 42 were collected at 12, 24, 48, 72, and 96 h)	Capillary: Fused silica. Voltage: +30 kV. Pressure: 25 mbar. BGE: 1 M FA and 10% (v/v) MeOH. IS: Methionine sulfone	**ESI(+)-TOF**. SL: 50% (v/v) MeOH −H$_2$O + reference masses	(L2) - m/z + RMT compared to in-house library	(&) - Post 24 h of HT, a stable disease scenario emerged characterized by 4−8% alterations in metabolic features related to lipid metabolism, cofactor and vitamin metabolism, glycan biosynthesis and metabolism, amino acid metabolism, and nucleotide metabolism.	[23]
28	Cell media (2021)	Respiratory allergies	$N = 18$ (Apical and basolateral cell media from calu-3 cells (line cell from lung adenocarcinoma patients) exposed to allergens Der p 1 or Ole e 1 and PBS at 2 and 7 days of growth, n = 3/group)	Capillary: Fused silica. Voltage: +30 kV. Pressure: 25 mbar. BGE: 1 M FA and 10% (v/v) MeOH. IS: Methionine sulfone	**ESI(+)-TOF**. SL: 50% (v/v) of MeOH −H$_2$O + reference masses	(L1) - spiking with standards (L3) - m/z	On day 2, L-glutamic acid, L-isoleucine, L-kynurenine, L-methionine, L-tyrosine, L-tryptophan, and L-valine were (↑) in the apical compartment after exposure to Der p 1. On other hand, on day 7, the (↑) metabolites were L-alanine, L-arginine, L-glycine, L-glutamine, L-glutamine, L-isoleucine, and L-methionine.	[63]
29	Human cells (2021)	Malignant pleural mesothelioma (MPM)	$N = 24$ (two cell lines: parental and resistant cells, treated with pemetrexed and controls, n = 6/group)	Capillary: Fused silica. Voltage: +30 kV, BGE: 1 M FA. IS: D-camphor-10-sulfonic acid Capillary: SMILE (+). Voltage: −30 kV, BGE: 50 mM NH$_4$Ac (pH 8.5). IS: D-camphor-10-sulfonic acid	**ESI(+)-TOF**. SL: 50% (v/v) of MeOH −H$_2$O + reference masses ESI(−)-TOF. SL: NH$_4$Ac (5 mM) in 50% (v/v) of MeOH −H$_2$O + reference masses	(L2) - m/z + RMT compared to standards	(↑) deoxyuridine monophosphate metabolite in pemetrexed-treated parental cell lines. On the other hand, deoxythymidine monophosphate was (↑) in the pemetrexed-treated resistant cell lines. Furthermore, deoxythymidine triphosphate was (↓) in both parental cell lines after PMX treatment.	[59]

Table 1 (*continued*)

8

No	Sample type (Year)	Disease	Sample size	CE conditions	MS conditions	Confidence level and ID	Significant metabolites (&)	Ref.
30	Human cells (2021)	Epithelial−mesenchymal transition (EMT)	$N = 24$ Non-small-cell lung cancer (NSCLC) cell lines (A549, HCC827, H358). Treated with transforming growth factor-β and controls (TGF-β) (n = 4/group)	Capillary: Fused silica. Voltage: +30 kV. BGE: 1 M FA. IS: Methionine sulfone, ethane sulfonic acid, and D-Camphor-10-sulfonic acid. Capillary: SMILE (+). Voltage: −30 kV. BGE: 50 mM NH$_4$Ac (pH 8.5). IS: Methionine sulfone, ethane sulfonic acid, and D-Camphor-10-sulfonic acid	**ESI(+)-TOF**. SL: 50% (v/v) of MeOH −H$_2$O + reference masses. **ESI(−)-TOF**. SL: NH$_4$Ac (5 mM) in 50% (v/v) of MeOH −H$_2$O + reference masses	(L1) - ID + QTF → m/z + MT compared to standards	The significant metabolites resulting from the comparison of TGF-β-treated and untreated cells were 49, 45 and 56 compounds for A549, H358 and HCC827 cells correspondingly. In A549 cells treated with TGF-β (↑) aspartic acid, glutamic acid, and lysine, and (↓) alanine, asparagine, citrulline, glutamine, glycine, histidine, hydroxyproline, isoleucine and leucine, proline, threonine and tyrosine.	[60]
31	Human cells (2021)	Tumor growth and metastasis	$N = 16$ Tumor (B16F10) and nontumor (ASF 4-1) cells treated with petasin (PT) or DMSO (n = 3/group)	Capillary: COSMO (+). Voltage: −30 kV. BGE: 50 mM NH$_4$Ac (pH 8.5). IS: Methionine sulfone, MES and D-camphor-10-sulfonic acid	**ESI(−)-TOF**. SL: NH$_4$Ac (5 mM) in 50% (v/v) of MeOH −H$_2$O + reference masses	(L1) - ID + QTF → m/z + RMT compared to standards	(↑) serine, asparagine, putrescine, and 4-methyl-2-oxopentanoate metabolites in PT-treated B16F10 cells. (↓) UTP, GTP, dCTP, ATP, S7P, UDP-glucose, CMP-Neu5Ac, UDP-GlcA, UDP-GlcNAc, aspartate, citrate, SAM$^+$ in B16F10 cells treated with PT.	[54]
32	Human cells (2021)	Breast cancer	$N =$ Not specified MCF-7-E10 breast carcinoma, type 1 (EDR1), type 2 (EDR2) cells	Capillary: Fused silica. Voltage: +30 kV. BGE: 1 M FA. IS: D-camphor-10-sulfonic acid. Capillary: SMILE (+). Voltage: −30 kV. BGE: 50 mM NH$_4$Ac (pH 8.5). IS: D-camphor-10-sulfonic acid	**ESI(+)-TOF**. SL: 50% (v/v) of MeOH −H$_2$O + reference masses. **ESI(−)-TOF**. SL: NH$_4$Ac (5 mM) in 50% (v/v) of MeOH −H$_2$O + reference masses	(L2) - m/z + MT compared to standards	(↑) leucine, isoleucine, methionine, histidine, tyrosine, tryptophan, phenylalanine, and valine in EDR1 and 2 cells compared to E10.	[61]
33	Human cells (2021)	Breast cancer	$N =$ Not specified MCF-7 cells Overexpression of LAT1 + MCF-7 Knockout of LAT1	Capillary: Fused silica. Voltage: +30 kV. BGE: 1 M FA. IS: Methionine sulfone, MES and D-camphor-10-sulfonic acid. Capillary: SMILE (+). Voltage: −30 kV. BGE: 50 mM NH$_4$Ac (pH 8.5). IS: Methionine sulfone, MES and D-camphor-10-sulfonic acid	**ESI(+)-TOF**. SL: 50% (v/v) MeOH −H$_2$O + reference masses. **ESI(−)-TOF**. SL: NH$_4$Ac (5 mM) in 50% (v/v) of MeOH −H$_2$O and reference masses	(L2) - m/z + RMT compared to standards	(↑) amino acid levels transported through LAT1: leucine, isoleucine, and valine.	[62]
34	Human cells (2021)	Cancer treatment with cisplatin	$N = 6$ Cisplatin (CDDP)-sensitive ovarian cancer A2780 cells + CDDP-resistant A2780cis cells (n = 3/group)	Capillary: Fused silica. Voltage: +30 kV. BGE: 1 M FA. IS: Methionine sulfone, MES and D-camphor-10-sulfonic acid. Capillary: COSMO (+). Voltage: −30 kV. BGE: 50 mM NH$_4$Ac (pH 8.5). IS: Methionine sulfone, MES and D-camphor-10-sulfonic acid	**ESI(+)-TOF**. SL: 50% (v/v) of MeOH −H$_2$O + reference masses. **ESI(−)-TOF**. SL: NH$_4$Ac (5 mM) in 50% (v/v) of MeOH −H$_2$O + reference masses	(L2) - m/z + RMT compared to standards	Glutamine, glutamate and glutathione levels were significantly higher in A2780cis cells than in A2780 cells.	[55]
35	Human cells (2019)	Prostatic cancer	Metabolization of [U−13C]-glucose up to very late time points (0 h, 0.25 h, 4 h, 12 h, 24 h, and long-term for 6 days performing thereby 3 passages) aiming to study the metabolic reaction in prostate tumor cells	Capillary: Fused silica. Voltage: +27 kV. BGE: 1 M FA. IS: not available. Capillary: COSMO (+). Voltage: −30 kV. Pressure: 15 mbar. BGE: 50 mM NH$_4$Ac (pH 8.5). IS: not available	**ESI(+)-TOF**. SL: 50% (v/v) of MeOH −H$_2$O + reference masses. **ESI(−)-TOF**. SL: NH$_4$Ac (5 mM) in 50% (v/v) MeOH −H$_2$O + reference masses	(L2) - m/z + MT compared to HMT library	(‡) UDP-GlcNAc and cystathionine were top listed as potential crucial metabolic node in prostate cancer cells. The mass isotopologue distribution data of UDP-GlcNAc may provide valuable clues for underlying metabolic anomalies.	[56]

#	Sample (year)	Cancer type	N / conditions	Capillary / Voltage / BGE / IS	MS	Identification	Findings	Ref
36	Human cells (2018)	Oral squamous cell carcinoma (OSCC)	N = 3 in each condition. OSCC cells and human oral cells (control). Cells were incubated for 60, 90, and 30 min with increasing concentrations of sodium-5,6-benzylidene-L-ascorbate (SBA), Benzaldehyde (BA), or sodium ascorbate (SA)	Capillary: Fused silica. Voltage: 30 kV. BGE: 1 M FA. IS: not available. Capillary: COSMO (+). Voltage: −30 kV. Pressure: 15 mbar. BGE: 50 mM NH$_4$Ac (pH 8.5). IS: not available	ESI(+)-TOF. SL: 50% (v/v) of MeOH −H$_2$O + reference masses. ESI(−)-TOF. SL: NH$_4$Ac (5 mM) in 50% (v/v) MeOH −H$_2$O + reference masses	(L2) - m/z + MT using standards from pre-sample analysis	Within 90 min exposure to BA, (↓) intracellular concentrations of citrate, cis-aconitate, and iso-citrate to base-line level in HSC-2 cells, whereas succinate, fumarate, and malate are constant.	[57]
37	Mice cells (2021)# (model transplanted subcutaneously with human SCLC cells with in vivo siRNA administration)	Small-cell lung carcinoma (SCLC)	N = 24 Two SCLC cell lines (DMS 273, NCI −H1048) with three different RRM1 inhibitions and a non-targeting siRNA (n = 3/ group)	Capillary: Fused silica. Voltage: +30 kV. BGE: 1 M FA. IS: Methionine sulfone, MES and D-camphor-10-sulfonic acid. Capillary: COSMO (+). Voltage: −30 kV. BGE: 50 mM NH$_4$Ac (pH 8.5). IS: Methionine sulfone, MES and D-camphor-10-sulfonic acid	ESI(+)-Orbitrap. SL: 50% (v/v) MeOH −H$_2$O + reference masses. ESI(−)-Orbitrap. SL: NH$_4$Ac (5 mM) in 50% of MeOH −H$_2$O + reference masses	(L2) - m/z + MT comparison with the HMT library	(&, ‡) - 427 metabolites were quantified in which ADP levels had similar concentrations in all groups. Inhibition of RRM1 (↓) deoxy-adenosine diphosphate and deoxyadenosine triphosphate level in both DMS 273 and H1048 cells.	[58]
38	Human saliva (2022)	Lung cancer and benign lung lesions	N = 63 (42 patients with lung cancer + 21 patients with benign lung lesions)	Capillary: Fused silica. Voltage: +30 kV. BGE: 1 M FA. IS: Methionine sulfone, MES and D-camphor-10-sulfonic acid, 3-aminopyrrolidine, and trimesate. Capillary: COSMO (+). Voltage: −30 kV. BGE: 50 mM NH$_4$Ac (pH 8.5). IS: Methionine sulfone, MES and D-camphor-10-sulfonic acid, 3-aminopyrrolidine, and trimesate	ESI(+)-TOF. SL: 50% (v/v) MeOH −H$_2$O + reference masses. ESI(−)-TOF. SL: NH$_4$Ac (5 mM) in 50% (v/v) of MeOH −H$_2$O + reference masses	(L1) - standards	(↓) tryptophan while (↑) choline, thymine, cytosine, phenylalanine leucine, isoleucine, lysine, and tyrosine in patients with lung cancer versus patients with benign lung lesions. Diethanolamine, cytosine, cytosine, lysine, and tyrosine were reported as potential biomarkers to distinguish lung cancer from benign lung lesions.	[24]
39	Human saliva (2021)	Colorectal cancer	N = 359 (276 patients with colorectal cancer, 26 patients with benign colorectal tumors, 57 healthy controls)	MSI-CE. Capillary: Fused silica. Voltage: +30 kV. BGE: 1 M FA. IS: creatinine-d3. Capillary: Fused silica. Voltage: 30 kV. BGE: 1 M FA. IS: creatinine-d3	ESI(+)-TOF. SL: 50% (v/v) of MeOH −H$_2$O + reference masses. ESI(+) -QqQ. SL: NH$_4$Ac (5 mM) in 50% (v/v) of MeOH −H$_2$O + reference masses	(L1) - standards + tandem MS/MS. (L1) - m/z + isotope-labeled standards	Biomarkers validation. Polyamines: spermidine, N$_1$-acetylspermidine, N$_8$-acetylspermidine, spermine, N$_1$, N$_8$-diacetylspermidine, N$_1$-acetylspermine and N$_1$, N$_{12}$-diacetylspermine.	[25]
40	Human saliva (2021)	Radiation therapy for head and Neck cancer	N = 36 (6 patients classified as low-grade + high-grade (3/ group), 4 sample collection times: before radiation therapy, during the 20 Gy dose, during the 40 Gy dose, and one week after the end of radiation therapy).	Capillary: Fused silica. Voltage: +30 kV. BGE: 1 M FA. IS: Methionine sulfone, MES and D-camphor-10-sulfonic acid, 3-aminopyrrolidine, and trimesate. Capillary: COSMO (+). Voltage: −30 kV. BGE: 50 mM NH$_4$Ac (pH 8.5). IS: Methionine sulfone, MES and D-camphor-10-sulfonic acid, 3-aminopyrrolidine, and trimesate	ESI(+)-TOF. SL: 50% (v/v) of MeOH −H$_2$O + reference masses. ESI(−)-TOF. SL: NH$_4$Ac (5 mM) in 50% (v/v) of MeOH −H$_2$O + reference masses	(L2) - m/z + RMT compared to standards	(↑) 3-aminoisobutyrate, 5-aminovalerate, cytosine guanine, histidine, tyrosine, homoserine, N,N-dimethylglycine, phenylalanine, and sarcosine in the high-grade group compared to the low-grade group during the four collection times. Of these, histidine and tyrosine highly discriminated high-grade from the low-grade group before initiation of radiotherapy. (↑) GABA and 2-aminobutyric acid levels in the high-grade group before radiotherapy.	[26]

Table 1 (continued)

No	Sample type (Year)	Disease	Sample size	CE conditions	MS conditions	Confidence level and ID	Significant metabolites (&)	Ref.
41	Human saliva (2019)	Patients with bone metastasis treatment with BMAs Osteonecrosis of the jaw (MRONJ)	N = 35 Screening cohort: Advanced MRONJ (n = 9) and controls (n = 9) Validation cohort: Advanced MRONJ (n = 8) and patients without MRONJ after the use of BMAs as a control group (n = 9)	Capillary: Fused silica. Voltage: +30 kV. BGE: 1 M FA. IS: not available Capillary: COSMO (+). Voltage: −30 kV. BGE: 50 mM NH₄Ac (pH 8.5). IS: not available	**ESI(+)-TOF**. SL: 50% (v/v) of MeOH −H₂O + reference masses **ESI(−)-TOF**. SL: NH₄Ac (5 mM) in 50% (v/v) MeOH −H₂O + reference masses	(L1) - m/z + RMT compared to standards + confirmed with standards	(↑) histamine, 3-(4-hydroxyphenyl) propionate, malonate, carnosine, and hypotaurine in the MRONJ group in the screening cohort. (↑) hypotaurine and malonate in MRONJ patients, although only hypotaurine was significant in the validation cohort.	[27]
42	Human tissue (2021)	Esophageal squamous cell carcinoma (ESCC)	N = 56 (ESCC tissues and paired para-cancer tissues from 28 ESCC patients)	Capillary: Fused silica. Voltage: +27 kV. BGE: 1 M FA. IS: Methionine sulfone and D-camphor-10-sulfonic acid (HMT, H3304-1002) Capillary: Fused silica. Voltage: +30 kV. BGE: 50 mM NH₄Ac (pH 8.5). IS: Methionine sulfone and D-camphor-10-sulfonic acid (HMT, H3304-1002)	**ESI(+)-TOF**. SL: 50% (v/v) of MeOH −H₂O + reference masses **ESI(+) -QqQ**. SL: 50% (v/v) of MeOH −H₂O + reference masses	(L2) - m/z + MT compared to the HMT library	(&, ‡) - (↑) choline, phosphocholine, CDP-choline, ethanolamine, phosphoethanolamine, phosphatidylethanolamine, S-adenosylmethionine, phosphatidylcholine, arginine, asparagine, aspartic acid, phenylalanine, proline, glutamic acid, glycine, histidine, lysine, methionine, tryptophan, tyrosine, serine, threonine, isoleucine, leucine, and valine in ESCC tissues compared to para-cancer tissue.	[50]
43	Human tissue (2020)	Gastric cancer (GC)	Cancer and adjacent non-cancerous tissues were obtained in a pair-wise manner from 140 patients with GC who underwent gastrectomy	Capillary: Fused silica. Voltage: +30 kV. BGE: 1 M FA. IS: not available Capillary: SMILE(+). Voltage: −30 kV. BGE: 50 mM NH₄Ac (pH 8.5). IS: not available	**ESI(+)-TOF**. SL: 50% (v/v) of MeOH −H₂O + reference masses **ESI(−)-TOF**. SL: NH₄Ac (5 mM) in 50% (v/v) MeOH −H₂O + reference masses	(L2) - m/z + MT compared to HMT library	(‡) (↑) lactate and (↓) the adenylate energy charge in cancer tissues compared to non-cancerous tissues. (↓) aspartic acid, β-alanine, GDP, and glycine levels in patients with recurrence than in those without.	[51]
44	Human tissue (2019)	Breast cancer	N = 20 Cluster-1: 5 benign, and 5 ductal carcinoma in situ (DCIS), and Cluster-2: 10 invasive ductal carcinoma (IDC)	**MSI-CE**. Capillary: Fused silica. Voltage: +30 kV. BGE: 1 M FA (pH 1.8). IS: not available **MSI-CE**. Capillary: Fused silica. Voltage: +30 kV. BGE: 50 mM NH₄Ac (pH 8.5). IS: not available	ESI(+)-TOF. SL: NH₄Ac (5 mM) in 50% (v/v) MeOH −H₂O **ESI(−)-TOF**. SL: NH₄Ac (5 mM) in 50% (v/v) MeOH −H₂O	(L1) - ID + QTF → using standards	(‡) Most affected pathways: pyrimidine, alanine, aspartate, glutamate, arginine, and proline pathways.	[52]
45	Human tissue (2018)	Esophageal cancer	N = 35 Paired tumor tissues (Ts) and non-tumor esophageal tissues (NTs), patients with T1 or T2 disease (pT1-2) and those with T3 or T4 disease (pT3-4))	Capillary: Fused silica. Voltage: +30 kV. BGE: 1 M FA. IS: H3304-1002, HMT Capillary: SMILE (+). Voltage: −30 kV. BGE: 50 mM NH₄Ac (pH 8.5). IS: PIPES	**ESI(+)-TOF**. SL: 50% (v/v) MeOH −H₂O + references masses **ESI(+)-TOF**. SL: NH₄Ac (5 mM) in 50% (v/v) MeOH −H₂O + reference masses	(L2) - m/z + RMT	(‡) (↑) lactate Ts, (↓) citrate Ts, (↓) malic acid and citric acid pT3-4 and (↓) asparagine and hydroxyproline.	[53]
46	Faeces (2022)	Fecal microbiota transplantation (FTM) as a treatment for recurrent Clostridioides difficile infection (rCDI)	N = 6 of one patient with (CDI) and with six episodes in total, samples were collected at (1st CDI, 3rd CDI, 0, 2, 8 and 23 weeks after FTM)	Capillary: Fused silica. Voltage: +30 kV. BGE: 1 M FA. IS: Methionine sulfone and 3-aminopyrrolidine	**ESI(+)-TOF**. SL: 50% (v/v) MeOH −H₂O + reference masses	(L2) - m/z + MT compared to the HMT library	(&, ‡) - 454 metabolites were detected including both techniques.	[120]

| 47 | Human *in vitro* fertilization embryo medium (2021) | Embryo preimplantation development | N = 40 (blastocyst stage embryos (day 4 or 5, n = 9); 8-cell stage embryos (day 3, n = 11; undeveloped embryos (n = 6); unfertilized oocytes (n = 5); control (medium with no embryos, n = 9)) | Capillary: Fused silica. Voltage: +30 kV. BGE: 15% acetic acid. IS: Methionine sulfone | **ESI(+)-TOF**. SL: 50% (v/v) MeOH $-H_2O$ + reference masses | (L1) - *m/z* + RMT compared to standards | Asparagine, aspartic acid, glutamic acid, isoleucine, proline, and tyrosine in unfertilized oocytes compared with the other groups. Asparagine and glutamine were associated with higher developmental stages of blastocyst stage. | [102] |
| 48 | Human bile (2021) | Pancreaticobiliary maljunction (PBM) | N = 10 (3 PBM patients without cancer of the biliary tract, 4 patients with extrahepatic bile duct cancer (EHBC) + 3 control patients with benign disease) | Capillary: Fused silica. Voltage: +30 kV. BGE: 15% acetic acid. IS: Methionine sulfone | **ESI(+)-TOF**. SL: 50% (v/v) MeOH $-H_2O$ + reference masses | (L2) - *m/z* + RMT compared to standards | Metabolites: isoleucine, phenylalanine, tyrosine, leucine, tryptophan, arginine, lysine, valine, asparagine, methionine, aspartic acid, serine, threonine, histidine, glutamine, alanine, proline, glutamic acid, and pyruvic acid were significant in PBM and EHBC patients compared to controls. | [103] |

Chemical abbreviations: IPA: isopropanol, ACN: acetonitrile, MeOH: methanol, IS: internal standard, SL: sheath liquid, MES: 2-(*N*-morpholino)ethanesulfonic acid, NH_4Ac: ammonium acetate, NH_4HCO_3: ammonium bicarbonate, NH_4OH: ammonium hydroxide, FA: formic acid.

Technique abbreviations: ID: identification and/or annotation, L, level of annotation by the compound identification work group of the Metabolomics Society [18,19], (&): metabolites reported from studies carried out using multiplatform (metabolites are not exclusively from CE-MS), #: studies in animals validated or related with human samples, (‡): semi-targeted metabolomic studies using the HMT services, ANNs: artificial neural networks, BGE: background electrolyte, ESI: electrospray ionization, HMT: Human Metabolome Technologies, MSI-NACE: multisegment injection-nonaqueous-capillary electrophoresis, MSI-CE: multisegment injection-capillary electrophoresis, MT: migration time, QTF: quantification, QqQ: triple quadrupole mass spectrometry, QTOF: quadrupole time-of-flight mass spectrometry, RMT: relative migration time, ISF: In-source fragmentation.

Metabolites abbreviations: ADMA: asymmetric dimethylarginine, ATP: adenosine 5′-triphosphate, CDP-choline: cytidine 5′-diphosphocholine, CMP-Neu5Ac: cytidine 5′-monophosphate-*N*-acetylneuraminic acid, dCTP: 2′-deoxycytidine 5′-triphosphate, GABA: gamma-aminobutyric acid, GTP: Guanosine 5′-triphosphate, LAT1: large amino acid transporter 1, NEFAs: non-esterified fatty acids, RRM1: ribonucleotide reductase catalytic subunit M1, S7P: sedoheptulose-7-phosphate, SAM: S-adenosylmethionine, SDMA: symmetric dimethylarginine, TOF: time-of-flight mass spectrometry, UDP-GlcA: uridine diphosphate glucuronic acid, UDP-GlcNAc: uridine 5′-diphospho-*N*-acetylglucosamine, UDP-glucose: uridine 5′-diphosphate glucose, UTP: uridine 5′-triphosphate, Arg-Va: arginyl-valine, Glu-Ala: glutamyl-alanine, Glu-Arg: glutamyl-arginine, Glu-hyp: glycyl-4-hydroxyproline, Glu-Lys/ɛ-Glu-Lys: glutamyl-lysine/epsilon-(gamma-glutamyl)-lysine, Lys-Asp: lysyl-aspartic acid, Ser-hyp: seryl-hydroxyproline, Thr-Ala: threoninyl-alanine, Val-Leu: valyl-leucine, Cys-Gly: cysteinyl-glycine, Cys-Gly disulfide: cysteinyl-glycine disulfide, Gly-Pro: glycyl-proline, Ser-Ala: seryl-alanine, Ser-Val: seryl-valine, Thr-Gly: threonyl-glycine, LAT1: L-type amino acid transporter 1, EDR: estrogen deprivation-resistant, ADP: adenosine 5′-diphosphate, UDP-GlcNAc: uridine diphosphate-*N*-acetylglucosamine, and GDP: guanosine 5′-diphosphate.

Disease and/or treatment abbreviations: SARS-CoV-2: severe acute respiratory syndrome coronavirus 2, PD: parkinson disease, NETs: neuroendocrine tumors, MetS: metabolic syndrome, CKD: chronic kidney disease, HCV: hepatitis C virus, NASH: nonalcoholic steatohepatitis, GDM: gestational diabetes mellitus, hPD-MSCs: human placenta-derived mesenchymal stem cells, AKI: acute kidney injury, CRC: colorectal cancer, IBD: inflammatory bowel disease, CD: Crohn's disease, UC: ulcerative colitis, NE: neonatal encephalopathy, HT: therapeutic hypothermia, PBS: phosphate-buffered saline, MPM: malignant pleural mesothelioma, MSI-CE: epithelial−mesenchymal transition, NSCLC: non-small-cell lung cancer, TGF-β: transforming growth factor-β, PT: petasin, DMSO: dimethylsulfoxide, CDDP: cisplatin, SCLC: small-cell lung carcinoma, Gy: unit of ionizing radiation dose, ESCC: esophageal squamous cell carcinoma, PBM: pancreaticobiliary maljunction, EHBC: extrahepatic bile duct cancer, CCA: cholangiocarcinoma, CF: cystic fibrosis, PKU: phenylketonuria, DCIS: ductal carcinoma in situ, IDC: invasive ductal carcinoma, MRONJ: medication-related osteonecrosis of the jaw, BMAs: bone-modifying agents, OSCC: oral squamous cell carcinoma, SBA: sodium-5,6-benzylidene-ʟ-ascorbate, SA: sodium ascorbate, BA: benzaldehyde, RA: rheumatoid arthritis, TNFi: TNF-a inhibitors, ABT: TNFi, CAD: coronary artery disease, OPLL: ossification of the posterior longitudinal ligament, GC: gastric cancer, VPI: very preterm infants, EUGR: extrauterine growth restricted, PAD: peripheral artery disease, PMX: pemetrexed, CLTI: chronic limb-threatening ischemia, IC: intermittent claudication, FTM: fecal microbiota transplantation, rCDI: recurrent Clostridioides difficile infection, OAB: overactive bladder, Ts: tumor tissues, NTs: non-tumor esophageal tissues, pT1-2: patients with T1 or T2 disease, and pT3-4: T3 or T4 disease. (↑): significantly increased metabolites, (↓): significantly decreased metabolites.

applications with capillary zone electrophoresis (CZE) are used, being normal polarity the most frequent by far. This methodology uses a fused silica capillary, applies a positive voltage, and uses an acidic BGE to separate highly polar metabolites that can be charged positively (cations). These metabolites are later analyzed in the MS using positive electrospray ionization (ESI+). As observed in Table 1, the 48 applications for cations followed this method. On the other hand, for the analysis of negatively charged metabolites (anions), the use of a basic BGE containing a salt of ammonium neutralizes anions by producing positively charged ammonium adducts which can be measured by ESI+. This methodology was employed in great part of the studies focused on anionic metabolites [22,31,37,39,43,44,49,50,52]. In this way, normal CE separation conditions were used for the analysis of anionic compounds. Other methodologies have been developed, such as the cationic polymer-coated capillaries COSMOS(+) [20,21,24,26,27,36,41,42,54−58] and SMILE(+) [32,34,45,47,51,53,59−62] with a negative voltage (reversed polarity). Both capillaries are coated with a cationic polymer so that the electroosmotic flow (EOF) goes from the cathode (−) to the anode (+). This leads the EOF in an opposite direction to non-coated capillaries in a pH-independent manner. With high reproducibility and a wide pH range of application, these capillaries allow the separation of anionic metabolites such as carboxylic acids, which migrate first when they are negatively charged. Both combinations are then detected in negative ESI mode (ESI-). Interestingly, a novel methodology using the polyvinyl alcohol (PVA) capillary and acidic BGE with negative voltage has been developed for analyzing anions and showed better results than the fused silica capillary method for anions [64]. Worthy of note is the fact that more than half of the studies listed in Table 1 reported the use of complementary modes of separation in CE-MS for the analysis of anions and cations metabolites (33 out of 48). This strategy allows to obtain a more complete picture of the polar/ionic part of the metabolome (Fig. 1B and C) [11,65,66]. Nonetheless, factors such as the BGE additives (e.g., the addition of organic solvents), pH conditions, voltage value, and pressure are adjusted uniquely in each methodology. In addition, other strategies, such as the derivatization with trimethylmethaneaminophenacetyl bromide, have been employed to increase the sensitivity and repeatability of metabolites in low concentrations and have enabled the analysis of carboxylic acid metabolites using normal polarity in CE [65].

3.3. Data treatment

For data treatment, as LC-MS, the pipeline for CE-MS typically consists of i) peak alignment, ii) peak picking, iii) filtering, iv) normalization, v) statistical analysis, and vi) metabolite annotation/identification (Fig. 1D) [67]. The main challenge when studying the metabolome is the extensive and complex data sets that are obtained after the experimental analysis. Consequently, user-friendly computational data processing tools are needed to reprocess the data and transform it into interpretable information. In comparison with LC-MS, to date, all open-source and commercial software tools are also helpful for CE-MS, with the difference in MT alignment [68]. MT shifting usually occurs due to the proteins or molecules that adhere to the capillary's inner wall during the worklist analysis. In addition, MT fluctuation strongly affects the peak alignment and feature-building steps, thus hindering the identification of unknown compounds. Consequently, a standardized approach is needed to align MTs in CE-MS, a key step to overlying the profiles. However, this limitation has been widely overcome in recent years with the development of new informatic tools that align and correct the low reproducibility of MTs [69,70]. This is the case of the software ROMANCE [71], a Python-based script by Huang et al. [72],

and the MobilityTransformR package [73], which were specifically created for CE-MS data [72,73]. Additionally, the vendor-software Agilent MassHunter Profinder 10.0 allows the users to perform electropherograms alignment [74].

Regarding the peak-picking process, it globally aims to find the comigrating ions corresponding to the same molecule, which are associated by their mass-to-charge ratio (m/z), charge-state, isotopic distribution, neutral loss (NL), dimmers, and/or the presence of adducts [70]. This latter aspect can come from BGE composition and/or the sample and it is a fundamental aspect to consider for CE-MS, as it is common to find many different adducts such as $[M+Na]^+$, $[M+K]^+$, and $[M + NH_4]^+$. For example, the addition of acetate or formate to the BGE for ESI(−)-MS will lead to the formation of $[M + CH_3COO]^-$ and $[M + HCOO]^-$ adducts with a mass difference of 60.0211 and 46.0054 Da, respectively, from the $[M − H]^-$ ion. This step entails great complexity due to the broad range of peak intensities, sometimes poor separation of compounds, and the resulting distorted peak shapes, leading to multiple misassignments, especially since some metabolites can also undergo in-source decay giving rise to multiple ion fragments [75].Traditional LC-MS data software such as XCMS, MS-DIAL, and MZmine can also be applied to CE-MS for all these workflow steps. In the case of XCMS, the peak picking and alignment combined with the Isotopologue Parameter Optimization (IPO) software can be used to avoid false-positive peaks [76]. In a recent study by Höcker et al., the authors carried out MT alignment using ROMANCE and then ran the data through MZmine and XCMS to reduce misalignment and false positive features [77]. Also available for the processing of CE-MS data is the web-based platform Metaboanalyst 5.0 [78], which offers an easy-to-use pipeline to carry out data processing from raw data to the putative annotation of the MS peaks considering mass accuracy, different adducts, and ion modes. Another online software is Metandem, for MS-isobaric labelling-based metabolomics, which provides a comprehensive pipeline for metabolite quantification, normalization, statistical analysis, and identification in the same software package. It is also the first omics data analysis software to include functionalities to execute online parameter optimization for customization. The developers demonstrated the tool's suitability for UHPLC−MS/MS, nano LC-MS/MS, CE-MS/MS, and matrix-assisted laser desorption/ionization (MALDI)-MS platforms [79]. Interestingly, a ROMANCE update showed the flexibility of uploading different data types and formats, measurement conditions, and the possibility of performing metabolite quantification [80]. Regarding the MobilityTransformR package [73], it allows the researcher to work with the data obtained in CE-MS directly in the programming language called R, saving the need for using multiple software.

In our experience, data filtration is essential to avoid signals that do not correspond precisely to metabolites. To this day, there is no software that can filtrate the compounds appearing together with the high concentration of salts that appear at the beginning of the electropherograms or assign the m/z values that correspond to fragments. Attempting to prove the robustness of CE-MS as a unique tool in metabolomics, a recent study proposed 13 independent laboratories spread across 11 countries in 2 continents to analyze the same batch of samples, which consisted of human plasma and urine spiked with the same representative metabolite mixture; and to compare relative MT (RMT) versus effective electrophoretic mobility (μ_{eff}) as criteria for metabolite annotation [81]. RMT is the result of a correction of MTs using an internal standard (IS) such as methionine sulfone, procaine, and paracetamol (additional IS can be observed in Table 1) [70]. The authors demonstrated that regardless of the massive heterogeneity in experimental conditions, instrumental platforms, and users involved in the trial, the conversion of MTs into μ_{eff} reduced variability below 10.9% and 3.1%
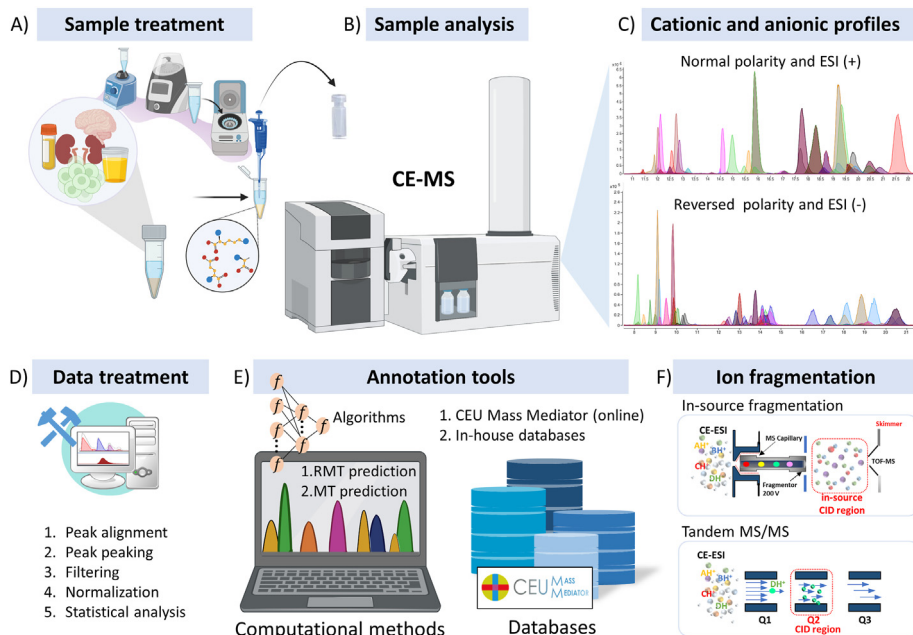
Fig. 1. Overview of CE-MS workflow for the untargeted analysis of polar and ionic metabolites. A) Diagram of sample treatment. B) Sample analysis showing the CE-MS instrumentation. C) Acquisition of cationic and anionic profiles in CE-MS. D) Data treatment steps. E) Annotation tools used for CE-MS; algorithms for RMT and MT prediction, and databases (online and in-house). F) Annotation obtained by the fragmentation pattern using in-source fragmentation and tandem MS/MS. Figure created with Biorender.com.

for RMT and μ_{eff}, respectively, maintaining a standardized condition of BGE.

Finally, the last step before biological interpretation is metabolite annotation. Given the importance of this step and the fact that it is crucial to obtain reliable results we will describe it in depth in the next section.

4. Metabolite annotation: Annotation tools in CE-MS for untargeted analysis

Currently, there are multiple databases to facilitate metabolite annotation. However, we can face two different and tricky scenarios during this process: we can obtain from dozens to thousands of potential candidates, or no match at all [67].The most common mass analyzers for CE-MS are the time of flight (TOF) and hybrid mass analyzers such as quadrupole TOF (QTOF). TOF provides high mass resolution and mass accuracy, allowing the elemental compositions of the metabolites to be determined from their isotopic patterns [69,82]. However, with the use of TOF in CE-MS, one of the main limitations was the impossibility of performing tandem mass spectrometry (MS/MS), and with QTOF, the MS/MS experiments with metabolites present in low quantities are hindered by the low sensitivity of the fragments [70]. This is why most CE-MS applications employ TOF (Table 1), and only a few use QTOF [20,39], Orbitrap [38,58] and triple quadruple (QqQ) [25,50] mass analyzers [2]. Besides mass accuracy, the traditional method for metabolite annotation in CE-MS has been the comparison of MTs or μ_{eff}, m/z values; and RMT of the metabolite in the sample with the authentic standard, both analyzed under the same analytical conditions. This annotation has then been confirmed by adding the standard to the sample and observing the increase of the corresponding peak. However, this method is not always possible to carry out due to the lack of commercial standards. All in all, new improvements in annotation by CE-MS have been developed recently and have led CE-MS to a more robust and promising technique [71,81,83] (Fig. 1E and F).

4.1. Computational alternatives and in-house libraries of effective electrophoretic mobility and relative migration time

Some researchers have developed different computational methods to predict MTs and RMTs of metabolites to assist in the annotation and identification process (Fig. 1E). Specifically, from 2005 to 2010, several research groups showed that their methods helped to annotate certain features (including low-abundance unknowns) to a candidate from an online database [84–86]. These prediction methods are based on algorithms such as artificial neural networks (ANNs), computational simulations (Hubbard-Onsager model and Simul 5.0), and support vector regression (SVR) (Fig. 1E). The most recent one has allowed to predict the MTs of up to 2938 compounds included in the Human Metabolome Database (HMDB) and has been validated using 375 standards, obtaining a correlation coefficient of 0.905 [86]. Then, in 2017, a chemo-informatic approach using random forest regression to identify unknown signals was presented [87]. This strategy allowed the annotation of 197 metabolites in human urine samples; both gly-cocyamidine and *N*-acetylglycine were described for the first time using this method.

Open-access data repositories for untargeted metabolomics are indispensable for metabolomics research (Fig. 1E). Soga and co-workers reported the first in-house library in 2003, showing experimental RMT values from 352 standards [88]. In 2018 and 2020, two research groups built up the mass spectrometry metabolite library by analysing multiple standards obtained from two commercial vendors (IROA technologies and Sigma-Aldrich) and published experimental μ_{eff} values for 276 and 458 compounds respectively, including xenobiotics and endogenous metabolites [81,89]. Two different CE-MS platforms and conditions were used in each study. In the first study, normal polarity in CE and positive ionization mode in a CE-ion trap-MS were used [89], whereas in the second one normal and reversed polarities in CE and positive and negative ionization modes in CE-QTOF-MS were employed [81]. The results of both in-house libraries were reported

in Excel files. In 2021, Mamani-Huanca et al. presented an in-house library containing RMTs and *m/z* values for 226 standards of purely endogenous metabolites showing the annotation for more than 2000 features obtained from their analysis, including in-source fragmentation information, multicharged ions, and adducts [83]. These were analyzed in normal polarity in CE and positive ionization mode in a CE-TOF-MS. All the obtained data were incorporated to the CEU Mass Mediator online tool under the "CE-MS *search*" section (Fig. 1E) [83].

4.2. In-source fragmentation as a tool for metabolite annotation

Using these computational tools and in-house experimental libraries help select the most likely candidate in the first tentative annotation step. However, annotation in untargeted metabolomic studies is much more complex. This is due to the presence of a large number of unknown signals [90,91] and the need for a high confidence level required for proper biological interpretation. While accurate mass enables the chemical characterization only at a formula level, tandem MS/MS experiments provide structural characterization. The information obtained from the MS/MS spectra allows rapid and accurate identification by comparing them to the MS/MS spectra of standards. However, these fragmentation libraries are still incomplete. Although computational methods have been developed to simulate MS/MS spectra by performing theoretical fragmentations (*in silico*), validation of the identification is necessary whenever it is possible [92].

Novel approaches have been developed to help in this matter. This is the case of the use of in-source fragmentation (ISF) for metabolite annotation (Fig. 1F). ISF, also known as in-source collision-induced dissociation (IS-CID), is an involuntary phenomenon that occurs naturally in the ionization sources at atmospheric pressure. This is the case of ESI, the most widely employed ionization source for LC-MS and CE-MS [93], and although it is considered one of the mildest ionization sources, it generates fragments from the parent ions. The ISF is the result of the vibrational excitation of ions produced in the intermediate pressure region between the atmospheric pressure source, and the inlet cone (skimmer) of the high vacuum of the MS [94]. Generally, the *m/z* signals produced by ISF belong to fragments, artifacts, and contaminants and these signals are often unknown because they are not considered in the annotation databases [95–98]. Although ISF cannot be avoided, it has been proved that the obtained fragment ions provide critical information for structural elucidation, mainly when single-stage mass analysers such as TOF are being used [99]. Moreover, this fragmentation can be forced intentionally by increasing the fragmentor voltage (e.g., 200 V), obtaining fragments for metabolite annotation. In this way, *pseudo*-MS/MS spectra produced by the ISF are demonstrated to be very similar to those obtained with typical MS/MS experiments at a QTOF [100]. In addition, these fragmentation patterns are independent of the biological matrix. It is crucial to consider that in ISF, the metabolite of interest cannot be isolated before fragmentation; consequently, the acquired spectrum contains numerous signals. Thus, data treatment is essential to obtain an accurate annotation, as Godzien et al. exemplified: they proposed a correlation method with the aim of clustering the fragment signals and their parent ion produced in ISF [101]. As observed in Table 1, most of the studies applied at least two or more experimental characteristics such as *m/z* or mass accuracy, RMT, tandem MS/MS or ISF to assign an annotation (Fig. 1E and F). Additionally, some studies reported the use of in-house libraries to carry out their metabolite annotation [28,29,31]. In any case, commercial standards are the main procedure used to confirm the identities of the metabolites [20–22,24–26,38,41–43, 54,55,59–62,102,103].

4.3. Example of new annotations in CE-MS: modified amino acids

One of the main objectives of untargeted metabolomic studies is the annotation of metabolites which are expressed differently in pathological conditions. For example, symmetric dimethylarginine (SDMA) and asymmetric dimethylarginine (ADMA) are metabolites associated with renal and cardiovascular disorders, respectively [104]. These metabolites arise from modifying an amino acid, specifically from the methylation of arginine [104]. Proteinogenic amino acids constitute the structure of proteins. These, in turn, undergo post-translational modifications (PTMs), and when these are degraded, they generate modified amino acids (MAAs) [105]. Consequently, MAAs are involved in different pathologies. Hence the importance of the identification of MAAs. However, these metabolites are often annotated as unknown because many of these amino acid modifications remain to be discovered.

In a recent study, a strategy for the identification of MAAs was developed. The workflow for annotation uses the analysis of a sample or quality control after the untargeted analysis worklist with higher fragmentation voltage (e.g., 200 V) in the fragmentor, because for fragment formation an excess of energy is required. This study extensively described the fragmentation mechanisms of 20 proteinogenic amino acids. The authors used characteristic ions, known in proteomics as diagnostic ions (DIs), for the unequivocal annotation of metabolites. In the case of the amino acids, these DIs are produced by sequential losses of H_2O and CO to eventually generate the immonium ion $[M + H-H_2O-CO]^{+}$ except for arginine and lysine. This way, specific ions were obtained for each modification of the amino acids and were characterized by the sum of the DI and the modification group. For example, for lysine methylation, the specific ion of *m/z* 98.0962 was observed, resulting from the sum of *m/z* 84.0811 (DI of lysine) plus the modification (methyl group 14.0157 Da); while for acetylation, the addition of the acetyl group to the DI (+42.0106 Da) was observed which provided a specific ion of *m/z* 126.0915. The new annotation of N_2-methyl-L-lysine demonstrated the potential of DIs for identifying MAAs and their differentiation from their lysine methylated isomer N_6-methyl-L-lysine in the kidney tissue of mice with urethral obstruction. From these, *m/z* 98.0962 showed to be more intense in N_2-methyl-L-lysine. Likewise, this strategy was applied to the methylated forms of arginine, where asymmetric *N,N*-dimethyl-L-arginine (ADMA) and symmetric *N,N′*-dimethyl-L-arginine (SDMA) were showed to have different RMT and DIs leading to an unequivocal annotation. In this sense, the methodology would allow the correct identification of these two isomers, in contrast to previously published literature where the identification is uncertain. This strategy led to the identification of *N*-methylproline, confirmed by the commercial standard, and *N-trans*-methylproline, which could not be confirmed due to the lack of a standard [106]. Another interesting example of this strategy was the characterization of argininosuccinic acid's open and cyclic forms (ASA), an immediate precursor of arginine, a substrate for urea, polyamines, creatine-phosphate, and nitric oxide production. These forms of ASA were not included previously in any database. In addition, the authors highlighted that, for the correct determination of total ASAs, the sum of all its forms should be considered to avoid the loss of information related to each ASA [107].

5. Future perspectives: Single cell-CE and CE-ion mobility (IM)-MS

CE-MS is a unique technique that various research groups have taken to a higher level of application, such as single-cell analysis and CE-IM-MS. Regarding single-cell metabolite profiling, the main limitation is sensitivity, as up to this moment there is no process

analogous to DNA amplification based on metabolites. However, using precision microcapillaries, light microscopy and CE-MS, researchers have succeeded in analysing single human cells such as HeLa (RCB0007) [108], rat neurons [109,110], *Aplysia californica* cells (from a sea slug) [111–114], and embryonic cells of *Xenopus laevis* (South African frog) [115–118]. In the case of HeLa cells, the study included the combination of the "nanoCESI" emitter with a large-volume dual preconcentration strategy. The nanoCESI enables sheathless ionization and minimizes the flow rate inside the capillary. In addition, the large-volume dual preconcentration sample is obtained by isotachophoresis and stacking, allowing an injection volume of 1200 nL. Thus, a higher sensitivity is reached than when using sheathless CE-MS alone [108].

There are various approaches for the use of a sheathless interface, which has the main advantage of increasing sensitivity with the same advantages as CE. With a sheathless interface it is possible to obtain broader coverage of the metabolomic profile of samples with low metabolite concentrations. Commercial capillaries made of bare fused-silica with a porous tip emitter are used for this purpose [115–117]. However, the robustness of this technology is under scrutiny. Therefore, it is necessary to continue working on the development of new interfaces that will help to increase the sensitivity of CE.

On the other hand, IM-MS is a technique based on the charge (z), shape, and volume of ions moving in the gas phase which calculates the cross-collisional section (CCS) of metabolites, providing additional selectivity to the MS. Here, the CCS values represent the effective area of the ion colliding with the molecules of a buffer gas (He or N_2). Serge Rudaz's group evaluated CCS in CE-IM-MS as complementary values for annotating metabolites in untargeted metabolomic studies. The authors analyzed a total of 482 compounds in ESI (+) and ESI (−) in normal and reversed polarity demonstrating that the μ_{eff} and CCS calculated with drift tube ion mobility spectrometry and nitrogen as buffer gas ($^{DT}CCS_{N2}$) values were highly reproducible. Their advantage was that the CCS values give an additional factor in the annotation. However, the coupling to IM causes a decrease in the signal, reducing the number of compounds detected by CE-MS [119].

6. Untargeted and semi-targeted metabolomics studies to approach disease diagnosis using CE-MS

Whenever a study aims to diagnose a disease, the biological sample is essential, and it is clear that less invasive samples continue to be the most explored, such as plasma [28–32], serum [38–43], and urine [20–22] (Table 1). This is because both blood and urine are either non-invasive or barely so, and can provide a stable matrix for the diagnosis. However, other interesting samples have been reported, such as cells [54,55,58–62], saliva [24–27], tissue [50–53], faeces [120], culture media [63], embryos [102], or bile [103,121]. In addition, the type of sample should match the disease.

The illnesses studied are very diverse. They can be broadly classified as cancer —the most analyzed disease— [20,24–26,30,50,54,55,58–62], metabolic-related disorders [31] including diseases such as gestational diabetes [38]; peripheral artery disease (PAD) [44], dietary interventions [36], and organ-related disorders such as lung [24,58,60,63] or brain [30] diseases. As described in section 4.3, we found several PTM metabolites reported, such as *N2*-methyllysine, which has been described in SARS-CoV-2 and advanced neuroendocrine tumors [28,30]. Other PTM metabolites such as 1-methyladenosine, dimethylglycine, N_2-methylproline, N_6-acetylhydroxylysine 3-methyl-2-oxovaleric acid, oxo-proline, *N,N*-dimethylglycine, N_1-acetylspermidine, N_8-acetylspermidine, N_1,N_8-diacetylspermidine, N_1-acetylspermine and N_1, N_{12}-diacetylspermine are also shown in Table 1, demonstrating how relevant this type of

metabolite is in the development of a disease. In addition, leucine and isoleucine have been reported to be altered significantly in various types of cancer, such as breast cancer [61,62], lung cancer [24,60] and oral squamous cell carcinoma (OSCC). Based on our experience, other amino acids, such as β-alanine, which was significant in gastric cancer, can be separated by CE-MS from α-alanine and sarcosine, all isomers. Similarly, the separation of citrate, *cis*-aconitate, and iso-citrate— statistically significant metabolites for OSCC [57], can be achieved using CE-MS. Another example is the analysis of GABA, which is significantly altered by radiotherapy in head and neck cancer [26]. This metabolite can be separated from its isomers [26] with this procedure.

An example of the maturity of the technique is the analysis of an increasing number of samples per study: 9 out of 48 studies included more than 100 samples [20,21,23,25,30,31,38,39,42]. 456 human plasma samples for metabolic syndrome (MetS) in early childhood [31]; 273 from pregnant women [38] and 590 in another study, also from pregnant women [39]; 729 samples for musculoskeletal disorders [42]; 284 and 359 samples for colorectal cancer in independent studies [20,25]; and 279 for neonatal encephalopathy [23].

From the analyses in Table 1 it is interesting to note that three studies —in pregnancy, non-alcoholic steatohepatitis, and PAD, reported the analysis of ionic lipids using this technique and showed phospholipids, bile acids, prostaglandins, fatty acids, and acylcarnitines as potential markers [38–40].

Among all these interesting applications of CE-MS for disease diagnosis collected in Table 1, we would like to highlight a study that used CE-MS for fluxomics, performing a stable-isotope tracing of [U−13C]-glucose in cells exposed to prostate cancer, showing the kinetics to up to 6 h for more than 30 metabolites, all related to energy and amino acid metabolism [56]. Interestingly, Human Metabolome Technology (HMT) offers CE-MS services using a semi-targeted methodology where, after obtaining the metabolomic profile, metabolites are collected using an in-house library of standards [34,37,45–48,51,56].

The study of the metabolome is complex because metabolites vary greatly in physicochemical properties and abundance. Different analytical techniques have been developed to cover as much as of the metabolome as possible. In this sense, CE-MS represents a unique platform that allows the study of polar and ionic metabolites in a complementary manner to other analytical techniques. CE-MS is a platform that has reached a steady state in untargeted analysis for the study of disease. To date, new tools have been created exclusively for the analysis of CE-MS data, although the traditional software tools for LC-MS have also been adapted to this platform. Finally, new ways to annotate metabolites in CE-MS have emerged, allowing the discovery of previously unknown metabolites and making CE-MS a reliable analytical platform in metabolomics. The MT shift characteristic of this technique requires more careful annotation using more than one feature (*m/z* and mass accuracy, RMT, MS/MS fragmentation, and/or ISF) for a reliable annotation. All in all, these facts have made CE-MS an essential platform capable of adding significant value to disease diagnosis research.

7. Conclusions

CE-MS is an analytical platform that has evolved in recent years to become a high-throughput method for untargeted metabolomics analysis. It has become a powerful complementary tool in the study of the metabolome and has been applied to the analysis of many types of samples including blood (plasma and serum), urine, cells, saliva, tissue, faeces and bile. In most cases, sample preparation is minimal. In addition, the analysis in two separation modes (normal

and reversed polarity) has increased the coverage of the polar and ionic metabolome. In terms of data treatment, increasing solutions have emerged to overcome the limitations of CE-MS, in particular MT shifting and metabolite annotation. The latter is a bottleneck in all untargeted metabolomic studies. Computational methods have been developed specifically for annotation in CE-MS, including algorithms for MT and RMT prediction, and databases (online and in-house) for putative annotation, have been created. These annotations have been validated by ion fragmentation using in-source fragmentation, an alternative method to tandem MS/MS for TOF-MS. Moreover, future directions point to the use of CE-MS in novel applications such as single-cell analysis and CE-IM-MS to increase isomer resolution and provide more accurate annotations. Its use in disease diagnosis has been demonstrated by the 48 research articles published in the last five years.

Author contributions (CRediT)

Maricruz Mamani-Huanca: Investigation, Data Curation, Writing - Review & Editing, Visualization. **Alma Villaseñor:** Investigation, Writing - Original Draft, Writing - Review & Editing, Visualization. **Carolina Gonzalez-Riano:** Investigation, Writing - Review & Editing, Visualization. **Ángeles López-López:** Investigation, Writing - Review & Editing, Visualization. **Ángeles Gonzálvez-López:** Investigation, Data Curation, Writing - Review & Editing, Visualization. **Coral Barbas:** Conceptualization, Writing - Review & Editing, Supervision, Project administration, Funding acquisition.

Declaration of competing interest

The authors declare that they have no known competing financial interests or personal relationships that could have appeared to influence the work reported in this paper.

Data availability

This is a review manuscript, all data were previously published

Acknowledgements

References

[1] U. Radzikowska, K. Baerenfaller, J.A. Cornejo-Garcia, C. Karaaslan, E. Barletta, B.E. Sarac, D. Zhakparov, A. Villaseñor, I. Eguiluz-Gracia, C. Mayorga, M. Sokolowska, C. Barbas, D. Barber, M. Ollert, T. Chivato, I. Agache, M.M. Escribese, Omics Technologies in Allergy and Asthma Research: an EAACI Position Paper, Allergy, 2022. https://doi.org/10.1111/all.15412. all.15412.
[2] D.S. Wishart, J. Godzien, A. Gil-de-la-Fuente, R. Mandal, R. Rajabzadeh, H. Pirimoghadam, C. Ladner-Keay, A. Otero, C. Barbas, CHAPTER 3. Metabolomics, in: R. Winkler (Editor), New Developments in Mass Spectrometry, Royal Society of Chemistry, Cambridge, 2020, pp. 41–95. https://doi.org/10.1039/9781788019880-00041.
[3] I. Gertsman, B.A. Barshop, Promises and pitfalls of untargeted metabolomics, J. Inherit. Metab. Dis. 41 (2018) 355–366. https://doi.org/10.1007/s10545-017-0130-7.
[4] X. Zhang, Q. Li, Z. Xu, J. Dou, Mass spectrometry-based metabolomics in health and medical science: a systematic review, RSC Adv. 10 (2020) 3092–3104. https://doi.org/10.1039/C9RA08985C.
[5] C. González-Riano, D. Dudzik, A. Garcia, A. Gil-de-la-Fuente, A. Gradillas, J. Godzien, Á. López-González, F. Rey-Stolle, D. Rojo, F.J. Ruperez, J. Saiz, C. Barbas, Recent developments along the analytical process for

[6] I. Aretz, D. Meierhofer, Advantages and pitfalls of mass spectrometry based metabolome profiling in systems biology, IJMS 17 (2016) 632. https://doi.org/10.3390/ijms17050632.
[7] A. Lioupi, M. Marinaki, C. Virgiliou, H. Gika, I. Wilson, G. Theodoridis, Chapter 1. State-of-the-art in LC−MS approaches for probing the polar metabolome, in: R. Ramautar (Editor), New Developments in Mass Spectrometry, Royal Society of Chemistry, Cambridge, 2021, pp. 1–26. https://doi.org/10.1039/9781839163524-00001.
[8] M.J. den Uijl, P.J. Schoenmakers, B.W.J. Pirok, M.R. Bommel, Recent applications of retention modelling in liquid chromatography, J. Separ. Sci. 44 (2021) 88–114. https://doi.org/10.1002/jssc.202000905.
[9] V. Sagi-Kiss, Y. Li, M.R. Carey, S.J. Grover, K. Siems, F. Cirulli, A. Berry, C. Musillo, I.D. Wilson, E.J. Want, J.G. Bundy, Ion-pairing chromatography and amine derivatization provide complementary approaches for the targeted LC-MS analysis of the polar metabolome, J. Proteome Res. 21 (2022) 1428–1437. https://doi.org/10.1021/acs.jproteome.2c00030.
[10] N.L. Kuehnbaum, P. Britz-McKibbin, New advances in separation science for metabolomics: resolving chemical diversity in a post-genomic era, Chem. Rev. 113 (2013) 2437–2468. https://doi.org/10.1021/cr300484s.
[11] W. Zhang, T. Hankemeier, R. Ramautar, Next-generation capillary electrophoresis−mass spectrometry approaches in metabolomics, Curr. Opin. Biotechnol. 43 (2017) 1–7. https://doi.org/10.1016/j.copbio.2016.07.002.
[12] M.G.M. Kok, G.W. Somsen, G.J. de Jong, Comparison of capillary electrophoresis−mass spectrometry and hydrophilic interaction chromatography−mass spectrometry for anionic metabolic profiling of urine, Talanta 132 (2015) 1–7. https://doi.org/10.1016/j.talanta.2014.08.047.
[13] D. Rojo, C. Barbas, Á. López-González, Metabolomics analysis of leishmania by capillary electrophoresis and mass spectrometry, in: E.E.K. Baidoo (Editor), Microbial Metabolomics, Springer, New York, 2019, pp. 253–260. https://doi.org/10.1007/978-1-4939-8757-3_14. New York, NY.
[14] H. Wu, K. Tang, Highly sensitive and robust capillary electrophoresis-electrospray ionization-mass spectrometry: interfaces, preconcentration techniques and applications, Rev. Anal. Chem. 39 (2020) 45–55. https://doi.org/10.1515/revac-2020-0112.
[15] Z. Gao, W. Zhong, Recent (2018−2020) development in capillary electrophoresis, Anal. Bioanal. Chem. 414 (2022) 115–130. https://doi.org/10.1007/s00216-021-03290-y.
[16] K. Klepárník, Recent advances in combination of capillary electrophoresis with mass spectrometry: methodology and theory: CE and CEC, Electrophoresis 36 (2015) 159–178. https://doi.org/10.1002/elps.201400392.
[17] W. Zhou, B. Zhang, Y. Liu, C. Wang, W. Sun, W. Li, Z. Chen, Advances in capillary electrophoresis-mass spectrometry for cell analysis, TrAC, Trends Anal. Chem. 117 (2019) 316–330. https://doi.org/10.1016/j.trac.2019.05.011.
[18] I. Blaženović, T. Kind, J. Ji, O. Fiehn, Software tools and approaches for compound identification of LC-MS/MS data in metabolomics, Metabolites 8 (2018) 31. https://doi.org/10.3390/metabo8020031.
[19] L.W. Sumner, A. Amberg, D. Barrett, M.H. Beale, R. Beger, C.A. Daykin, T.W.-M. Fan, O. Fiehn, R. Goodacre, J.L. Griffin, T. Hankemeier, N. Hardy, J. Harnly, R. Higashi, J. Kopka, A.N. Lane, J.C. Lindon, P. Marriott, A.W. Nicholls, M.D. Reily, J.J. Thaden, M.R. Viant, Proposed minimum reporting standards for chemical analysis: chemical analysis working group (CAWG) metabolomics standards initiative (MSI), Metabolomics 3 (2007) 211–221. https://doi.org/10.1007/s11306-007-0082-2.
[20] T. Sakurai, K. Katsumata, R. Udo, T. Tago, K. Kasahara, J. Mazaki, H. Kuwabara, H. Kawakita, M. Enomoto, T. Ishizaki, Y. Nemoto, Y. Osaka, Y. Nagakawa, M. Sugimoto, A. Tsuchida, Validation of urinary charged metabolite profiles in colorectal cancer using capillary electrophoresis-mass spectrometry, Metabolites 12 (2022) 59. https://doi.org/10.3390/metabo12010059.
[21] R. Saito, A. Hirayama, A. Akiba, Y. Kamei, Y. Kato, S. Ikeda, B. Kwan, L. Natarajan, H. Shinjo, S. Akiyama, M. Tomita, T. Soga, S. Maruyama, Urinary metabolome analyses of patients with acute kidney injury using capillary electrophoresis-mass spectrometry, Metabolites 11 (2021) 671. https://doi.org/10.3390/metabo11100671.
[22] M. Yamamoto, M. Shanmuganathan, L. Hart, N. Pai, P. Britz-McKibbin, Urinary metabolites enable differential diagnosis and therapeutic monitoring of pediatric inflammatory bowel disease, Metabolites 11 (2021) 245. https://doi.org/10.3390/metabo11040245.
[23] J.D. Piñeiro-Ramos, M.M. Cascant, A. Núñez-Ramiro, Á. López-Gonzálvez, Á. Solaz-García, A. Albiach-Delgado, J. Martínez-Rodilla, R. Llorens-Salvador, D. Sanjuan-Herraez, G. Quintás, C. Barbas, J. Kuligowski, M. Vento, On behalf of the Hypotop Study Group, Noninvasive monitoring of evolving urinary metabolic patterns in neonatal encephalopathy, Pediatr. Res. 91 (2022) 598–605. https://doi.org/10.1038/s41390-021-01553-z.
[24] S. Takamori, S. Ishikawa, J. Suzuki, H. Oizumi, T. Uchida, S. Ueda, K. Edamatsu, M. Iino, M. Sugimoto, Differential diagnosis of lung cancer and benign lung lesion using salivary metabolites: a preliminary study, Thoracic Cancer 13 (2022) 460–465. https://doi.org/10.1111/1759-7714.14282.
[25] K. Igarashi, S. Ota, M. Kaneko, A. Hirayama, M. Enomoto, K. Katumata, M. Sugimoto, T. Soga, High-throughput screening of salivary polyamine markers for discrimination of colorectal cancer by multisegment injection capillary electrophoresis tandem mass spectrometry, J. Chromatogr. A 1652 (2021), 462355. https://doi.org/10.1016/j.chroma.2021.462355.

[26] W. Yatsuoka, T. Ueno, K. Miyano, A. Enomoto, S. Ota, M. Sugimoto, Y. Uezono, Time-course of salivary metabolomic profiles during radiation therapy for head and neck cancer, JCM 10 (2021) 2631. https://doi.org/10.3390/jcm10122631.

[27] W. Yatsuoka, T. Ueno, K. Miyano, Y. Uezono, A. Enomoto, M. Kaneko, S. Ota, T. Soga, M. Sugimoto, T. Ushijima, Metabolomic profiling reveals salivary hypotaurine as a potential early detection marker for medication-related osteonecrosis of the jaw, PLoS One 14 (2019), e0220712. https://doi.org/10.1371/journal.pone.0220712.

[28] O.E. Albóniga, D. Jiménez, M. Sánchez-Conde, P. Vizcarra, R. Ron, S. Herrera, J. Martínez-Sanz, E. Moreno, S. Moreno, C. Barbas, S. Serrano-Villar, Metabolic snapshot of plasma samples reveals new pathways implicated in SARS-CoV-2 pathogenesis, J. Proteome Res. 21 (2022) 623–634. https://doi.org/10.1021/acs.jproteome.1c00786.

[29] C. Gonzalez-Riano, J. Saiz, C. Barbas, A. Bergareche, J.M. Huerta, E. Ardanaz, M. Konjevod, E. Mondragon, M.E. Erro, M.D. Chirlaque, E. Abilleira, F. Goñi-Irigoyen, P. Amiano, Prognostic biomarkers of Parkinson's disease in the Spanish EPIC cohort: a multiplatform metabolomics approach, Npj Parkinsons Dis. 7 (2021) 73. https://doi.org/10.1038/s41531-021-00216-4.

[30] B. Soldevilla, A. López-López, A. Lens-Pardo, C. Carretero-Puche, A. Lopez-Gonzalvez, A. La Salvia, B. Gil-Calderon, M.C. Riesco-Martinez, P. Espinosa-Olarte, J. Sarmentero, B. Rubio-Cuesta, R. Rincón, C. Barbas, R. Garcia-Carbonero, Comprehensive plasma metabolomic profile of patients with advanced neuroendocrine tumors (NETs). Diagnostic and biological relevance, Cancers 13 (2021) 2634. https://doi.org/10.3390/cancers13112634.

[31] S.M. Azab, R.J. de Souza, A. Lamri, M. Shanmuganathan, Z. Kroezen, K.M. Schulze, D. Desai, N.C. Williams, K.M. Morrison, S.A. Atkinson, K.K. Teo, P. Britz-McKibbin, S.S. Anand, Metabolite profiles and the risk of metabolic syndrome in early childhood: a case-control study, BMC Med. 19 (2021) 292. https://doi.org/10.1186/s12916-021-02162-7.

[32] N. Motoki, H. Motoki, M. Utsumi, S. Yamazaki, H. Obinata, K. Takei, S. Yasukochi, Identification of metabolomic profile related to adult Fontan pathophysiology, IJC Heart & Vasculature 37 (2021), 100921. https://doi.org/10.1016/j.ijcha.2021.100921.

[33] D. Dudzik, I. Iglesias Platas, M. Izquierdo Renau, C. Balcells Esponera, B. del Rey Hurtado de Mendoza, C. Lerin, M. Ramón-Krauel, C. Barbas, Plasma metabolome alterations associated with extrauterine growth restriction, Nutrients 12 (2020) 1188. https://doi.org/10.3390/nu12041188.

[34] T. Tsuji, M. Matsumoto, M. Nakamura, T. Miyamoto, M. Yagi, N. Fujita, E. Okada, N. Nagoshi, O. Tsuji, K. Watanabe, Metabolite profiling of plasma in patients with ossification of the posterior longitudinal ligament, J. Orthop. Sci. 23 (2018) 878–883. https://doi.org/10.1016/j.jos.2018.07.001.

[35] M.P. Cala, M.T. Agulló-Ortuño, E. Prieto-García, C. González-Riano, L. Parrilla-Rubio, C. Barbas, C.V. Díaz-García, A. García, C. Pernaut, J. Adeva, M.C. Riesco, F.J. Rupérez, J.A. Lopez-Martin, Multiplatform plasma fingerprinting in cancer cachexia: a pilot observational and translational study, J. Cachexia Sarcopenia Muscle 9 (2018) 348–357. https://doi.org/10.1002/jcsm.12270.

[36] J. Wild, M. Shanmuganathan, M. Hayashi, M. Potter, P. Britz-McKibbin, Metabolomics for improved treatment monitoring of phenylketonuria: urinary biomarkers for non-invasive assessment of dietary adherence and nutritional deficiencies, Analyst 144 (2019) 6595–6608. https://doi.org/10.1039/C9AN01642B.

[37] C. Sasaki, T. Hiraishi, T. Oku, K. Okuma, K. Suzumura, M. Hashimoto, H. Ito, I. Aramori, Y. Hirayama, Metabolomic approach to the exploration of biomarkers associated with disease activity in rheumatoid arthritis, PLoS One 14 (2019), e0219400. https://doi.org/10.1371/journal.pone.0219400.

[38] S.M. Azab, R.J. de Souza, R. Ly, K.K. Teo, S.A. Atkinson, K.M. Morrison, S.S. Anand, P. Britz-McKibbin, Non-esterified fatty acids as biomarkers of diet and glucose homeostasis in pregnancy, The impact of fatty acid reporting methods, Prostaglandins, Leukotrienes and Essential Fatty Acids 176 (2022), 102378. https://doi.org/10.1016/j.plefa.2021.102378.

[39] C. Sikorski, S. Azab, R.J. de Souza, M. Shanmuganathan, D. Desai, K. Teo, S.A. Atkinson, K. Morrison, M. Gupta, P. Britz-McKibbin, S.S. Anand, Serum metabolomic signatures of gestational diabetes in South Asian and white European women, BMJ Open Diab. Res. Care 10 (2022), e002733. https://doi.org/10.1136/bmjdrc-2021-002733.

[40] R. Ly, N. Ly, K. Sasaki, M. Suzuki, K. Kami, Y. Ohashi, P. Britz-McKibbin, Nontargeted serum lipid profiling of nonalcoholic steatohepatitis by multi-segment injection—nonaqueous capillary electrophoresis—mass spectrometry: a multiplexed separation platform for resolving ionic lipids, J. Proteome Res. 21 (2022) 768–777. https://doi.org/10.1021/acs.jproteome.1c00682.

[41] Y. Akiyama, K. Kikuchi, T. Toyohara, E. Mishima, C. Suzuki, T. Suzuki, M. Nakayama, Y. Tomioka, T. Soga, T. Abe, CE-MS-Based identification of uremic solutes specific to hemodialysis patients, Toxins 13 (2021) 324. https://doi.org/10.3390/toxins13050324.

[42] K. Miyamoto, A. Hirayama, Y. Sato, S. Ikeda, M. Maruyama, T. Soga, M. Tomita, M. Nakamura, M. Matsumoto, N. Yoshimura, T. Miyamoto, A metabolic profile predictive of new osteoporosis or sarcopenia development, Metabolites 11 (2021) 278. https://doi.org/10.3390/metabo11050278.

[43] M. Shanmuganathan, M.O. Sarfaraz, Z. Kroezen, H. Philbrick, R. Poon, A. Don-Wauchope, M. Puglia, D. Wishart, P. Britz-McKibbin, A cross-platform metabolomics comparison identifies serum metabolite signatures of liver fibrosis progression in chronic hepatitis C patients, Front. Mol. Biosci. 8 (2021), 676349. https://doi.org/10.3389/fmolb.2021.676349.

[44] S.M. Azab, A. Zamzam, M.H. Syed, R. Abdin, M. Qadura, P. Britz-McKibbin, Serum metabolic signatures of chronic limb-threatening ischemia in patients with peripheral artery disease, JCM 9 (2020) 1877. https://doi.org/10.3390/jcm9061877.

[45] S. Takahashi, J. Saegusa, A. Onishi, A. Morinobu, Biomarkers identified by serum metabolomic analysis to predict biologic treatment response in rheumatoid arthritis patients, Rheumatology 58 (2019) 2153–2161. https://doi.org/10.1093/rheumatology/kez199.

[46] K. Omori, N. Katakami, Y. Yamamoto, H. Ninomiya, M. Takahara, T. Matsuoka, T. Bamba, E. Fukusaki, I. Shimomura, Identification of metabolites associated with onset of CAD in diabetic patients using CE-MS analysis: a pilot study, J. Atherosclerosis Thromb. 26 (2019) 233–245. https://doi.org/10.5551/jat.42945.

[47] H. Shimura, T. Mitsui, S. Kira, T. Ihara, N. Sawada, H. Nakagomi, T. Miyamoto, S. Tsuchiya, M. Kanda, M. Takeda, Metabolomic analysis of overactive bladder in male patients: identification of potential metabolite biomarkers, Urology 118 (2018) 158–163. https://doi.org/10.1016/j.urology.2018.05.001.

[48] S. Kira, T. Mitsui, T. Miyamoto, T. Ihara, H. Nakagomi, Y. Hashimoto, H. Takamatsu, M. Tanahashi, M. Takeda, N. Sawada, M. Takeda, Metabolomics analysis of blood identifies potential biomarkers and possible treatment targets for nocturia, Therapeutic Adv. Urol. 11 (2019), 175628721985008. https://doi.org/10.1177/1756287219850087.

[49] K.-H. Kim, K.-A. Lee, Metabolic rewiring by human placenta-derived mesenchymal stem cell therapy promotes rejuvenation in aged female rats, IJMS 23 (2022) 566. https://doi.org/10.3390/ijms23010566.

[50] B. Zang, W. Wang, Y. Wang, P. Li, T. Xia, X. Liu, D. Chen, H. Piao, H. Qi, Y. Ma, Metabolomic characterization reveals ILF2 and ILF3 affected metabolic adaptions in esophageal squamous cell carcinoma, Front. Mol. Biosci. 8 (2021), 721990. https://doi.org/10.3389/fmolb.2021.721990.

[51] S. Kaji, T. Irino, M. Kusuhara, M. Makuuchi, Y. Yamakawa, M. Tokunaga, Y. Tanizawa, E. Bando, T. Kawamura, K. Kami, Y. Ohashi, S. Zhang, H. Orita, H.-C. Lee-Okada, T. Fukunaga, M. Terashima, Metabolomic profiling of gastric cancer tissues identified potential biomarkers for predicting peritoneal recurrence, Gastric Cancer 23 (2020) 874–883. https://doi.org/10.1007/s10120-020-01065-5.

[52] N. Harada-Shoji, T. Soga, H. Tada, M. Miyashita, M. Harada, G. Watanabe, Y. Hamanaka, A. Sato, T. Suzuki, T. Ishida, A metabolic profile of routine needle biopsies identified tumor type specific metabolic signatures for breast cancer stratification: a pilot study, Metabolomics 15 (2019) 147. https://doi.org/10.1007/s11306-019-1610-6.

[53] M. Tokunaga, K. Kami, S. Ozawa, J. Oguma, A. Kazuno, H. Miyachi, Y. Ohashi, M. Kusuhara, M. Terashima, Metabolome analysis of esophageal cancer tissues using capillary electrophoresis-time-of-flight mass spectrometry, Int. J. Oncol. (2018). https://doi.org/10.3892/ijo.2018.4340.

[54] K. Heishima, N. Sugito, T. Soga, M. Nishikawa, Y. Ito, R. Honda, Y. Kuranaga, H. Sakai, R. Ito, T. Nakagawa, H. Ueda, Y. Akao, Petasin potently inhibits mitochondrial complex I—based metabolism that supports tumor growth and metastasis, J. Clin. Invest. 131 (2021), e139933. https://doi.org/10.1172/JCI139933.

[55] J. Guo, K. Satoh, S. Tabata, M. Mori, M. Tomita, T. Soga, Reprogramming of glutamine metabolism via glutamine synthetase silencing induces cisplatin resistance in A2780 ovarian cancer cells, BMC Cancer 21 (2021) 174. https://doi.org/10.1186/s12885-021-07879-5.

[56] J. Zeng, Z. Wang, X. Huang, S.S. Eckstein, X. Lin, H. Piao, C. Weigert, P. Yin, R. Lehmann, G. Xu, Comprehensive profiling by non-targeted stable isotope tracing capillary electrophoresis-mass spectrometry: a new tool complementing metabolomic analyses of polar metabolites, Chem. Eur. J. 25 (2019) 5427–5432. https://doi.org/10.1002/chem.201900539.

[57] H. Sakagami, M. Sugimoto, Y. Kanda, Y. Murakami, O. Amano, J. Saitoh, A. Kochi, Changes in metabolic profiles of human oral cells by benzylidene ascorbates and eugenol, Medicines 5 (2018) 116. https://doi.org/10.3390/medicines5040116.

[58] A. Maruyama, Y. Sato, J. Nakayama, J. Murai, T. Ishikawa, T. Soga, H. Makinoshima, De novo deoxyribonucleotide biosynthesis regulates cell growth and tumor progression in small-cell lung carcinoma, Sci. Rep. 11 (2021), 13474. https://doi.org/10.1038/s41598-021-92948-9.

[59] Y. Sato, M. Tomita, T. Soga, A. Ochiai, H. Makinoshima, Upregulation of thymidylate synthase induces pemetrexed resistance in malignant pleural mesothelioma, Front. Pharmacol. 12 (2021), 718675. https://doi.org/10.3389/fphar.2021.718675.

[60] F. Nakasuka, S. Tabata, T. Sakamoto, A. Hirayama, H. Ebi, T. Yamada, K. Umetsu, M. Ohishi, A. Ueno, H. Goto, M. Sugimoto, Y. Nishioka, Y. Yamada, M. Tomita, A.T. Sasaki, S. Yano, T. Soga, TGF-β-dependent reprogramming of amino acid metabolism induces epithelial—mesenchymal transition in non-small cell lung cancers, Commun. Biol. 4 (2021) 782. https://doi.org/10.1038/s42003-021-02323-7.

[61] H. Shindo, N. Harada-Shoji, A. Ebata, M. Sato, T. Soga, M. Miyashita, H. Tada, M. Kawai, S. Kosaka, K. Onuki, S. Usami, S. Furumoto, S. Hayashi, T. Abe, T. Suzuki, T. Ishida, H. Sasano, Targeting amino acid metabolic reprogramming via L-type amino acid transporter 1 (LAT1) for endocrine-resistant breast cancer, Cancers 13 (2021) 4375. https://doi.org/10.3390/cancers13174375.

[62] M. Sato, N. Harada-Shoji, T. Toyohara, T. Soga, M. Itoh, M. Miyashita, H. Tada, M. Amari, N. Anzai, S. Furumoto, T. Abe, T. Suzuki, T. Ishida, H. Sasano, L-type amino acid transporter 1 is associated with chemoresistance in breast cancer via the promotion of amino acid metabolism, Sci. Rep. 11 (2021) 589. https://

doi.org/10.1038/s41598-020-80668-5.

[63] J.C. López-Rodríguez, J. Rodríguez-Coira, S. Benedé, C. Barbas, D. Barber, M.T. Villalba, M.M. Escribese, A. Villaseñor, E. Batanero, Comparative metabolomics analysis of bronchial epithelium during barrier establishment after allergen exposure, Clin. Transl. Allergy 11 (2021). https://doi.org/10.1002/clt2.12051.

[64] Á. López-López, M. Ciborowski, J. Niklinski, C. Barbas, Á. López-Gonzálvez, Optimization of capillary electrophoresis coupled to negative mode electrospray ionization-mass spectrometry using polyvinyl alcohol coated capillaries. Application to a study on non-small cell lung cancer, Anal. Chim. Acta 1226 (2022), 340259. https://doi.org/10.1016/j.aca.2022.340259.

[65] M. Mever, C.C.W. Willacey, W. Zhang, N. Drouin, A.E. Christina, P.W. Lindenburg, J.P.D. Veldhoven, D. Es, A.C. Harms, T. Hankemeier, R. Ramautar, Profiling acidic metabolites by capillary electrophoresis-mass spectrometry in low numbers of mammalian cells using a novel chemical derivatization approach, Anal. Sci. Adv. 3 (2022) 3–13. https://doi.org/10.1002/ansa.202100054.

[66] M. Mever, T. Hankemeier, R. Ramautar, CE–MS for anionic metabolic profiling: an overview of methodological developments, Electrophoresis (2019), 201900115. https://doi.org/10.1002/elps.201900115. elps.

[67] S. Alseekh, A. Aharoni, Y. Brotman, K. Contrepois, J. D'Auria, J. Ewald, J.C. Ewald, P.D. Fraser, P. Giavalisco, R.D. Hall, M. Heinemann, H. Link, J. Luo, S. Neumann, J. Nielsen, L. Perez de Souza, K. Saito, U. Sauer, F.C. Schroeder, S. Schuster, G. Siuzdak, A. Skirycz, L.W. Sumner, M.P. Snyder, H. Tang, T. Tohge, Y. Wang, W. Wen, S. Wu, G. Xu, N. Zamboni, A.R. Fernie, Mass spectrometry-based metabolomics: a guide for annotation, quantification and best reporting practices, Nat. Methods 18 (2021) 747–756. https://doi.org/10.1038/s41592-021-01197-1.

[68] K. O'Shea, B.B. Misra, Software tools, databases and resources in metabolomics: updates from 2018 to 2019, Metabolomics 16 (2020) 36. https://doi.org/10.1007/s11306-020-01657-3.

[69] Y. Jiang, M.-Y. He, W.-J. Zhang, P. Luo, D. Guo, X. Fang, W. Xu, Recent advances of capillary electrophoresis-mass spectrometry instrumentation and methodology, Chin. Chem. Lett. 28 (2017) 1640–1652. https://doi.org/10.1016/j.cclet.2017.05.008.

[70] J. Godzien, Á. López-Gonzálvez, A. García, C. Barbas, Metabolic phenotyping using capillary electrophoresis mass spectrometry, in: The Handbook of Metabolic Phenotyping, Elsevier, 2019, pp. 171–204. https://doi.org/10.1016/B978-0-12-812293-8.00005-0.

[71] V. González-Ruiz, Y. Gagnebin, N. Drouin, S. Codesido, S. Rudaz, J. Schappler, ROMANCE: a new software tool to improve data robustness and feature identification in CE-MS metabolomics, Electrophoresis 39 (2018) 1222–1232. https://doi.org/10.1002/elps.201700427.

[72] Z. Huang, J. Tan, Y. Li, S. Miao, K.B. Scotland, B.H. Chew, D. Lange, D.D.Y. Chen, Migration time correction for dual pressure capillary electrophoresis in semi-targeted metabolomics study, Electrophoresis (2022), 202100365. https://doi.org/10.1002/elps.202100365.

[73] L. Salzer, M. Witting, P. Schmitt-Kopplin, MobilityTransformR: an R package for effective mobility transformation of CE-MS data, Bioinformatics (2022). https://doi.org/10.1093/bioinformatics/btac441. btac441.

[74] J.C. Reijenga, J.H.P.A. Martens, A. Giuliani, M. Chiari, Pherogram normalization in capillary electrophoresis and micellar electrokinetic chromatography analyses in cases of sample matrix-induced migration time shifts, J. Chromatogr. B 770 (2002) 45–51. https://doi.org/10.1016/S0378-4347(01)00527-8.

[75] W. Lu, X. Xing, L. Wang, L. Chen, S. Zhang, M.R. McReynolds, J.D. Rabinowitz, Improved annotation of untargeted metabolomics data through buffer modifications that shift adduct mass and intensity, Anal. Chem. 92 (2020) 11573–11581. https://doi.org/10.1021/acs.analchem.0c00985.

[76] M. Çelebier, M. Nenni, Recent developments in CE-MS based metabolomics, CAC 17 (2021) 1229–1242. https://doi.org/10.2174/1573411016999200709133339.

[77] O. Höcker, D. Flottmann, T.C. Schmidt, C. Neusüß, Non-targeted LC-MS and CE-MS for biomarker discovery in bioreactors: influence of separation, mass spectrometry and data processing tools, Sci. Total Environ. 798 (2021), 149012. https://doi.org/10.1016/j.scitotenv.2021.149012.

[78] Z. Pang, J. Chong, G. Zhou, D.A. de Lima Morais, L. Chang, M. Barrette, C. Gauthier, P.-É. Jacques, S. Li, J. Xia, MetaboAnalyst 5.0: narrowing the gap between raw spectra and functional insights, Nucleic Acids Res. 49 (2021) W388. https://doi.org/10.1093/nar/gkab382. –W396.

[79] L. Hao, Y. Zhu, P. Wei, J. Johnson, A. Buchberger, D. Frost, W.J. Kao, L. Li, Metandem: an online software tool for mass spectrometry-based isobaric labeling metabolomics, Anal. Chim. Acta 1088 (2019) 99–106. https://doi.org/10.1016/j.aca.2019.08.046.

[80] S. Codesido, N. Drouin, S. Ferre, J. Schappler, S. Rudaz, V. González-Ruiz, A mature ROMANCE: a matter of quantity and how two can Be better than one, Chemistry (2020). https://doi.org/10.26434/chemrxiv.12287048.v1.

[81] N. Drouin, J. Pezzatti, Y. Gagnebin, V. González-Ruiz, J. Schappler, S. Rudaz, Effective mobility as a robust criterion for compound annotation and identification in metabolomics: toward a mobility-based library, Anal. Chim. Acta 1032 (2018) 178–187. https://doi.org/10.1016/j.aca.2018.05.063.

[82] M. Schwaiger-Haber, E. Stancliffe, V. Arends, B. Thyagarajan, M. Sindelar, G.J. Patti, A workflow to perform targeted metabolomics at the untargeted scale on a triple quadrupole mass spectrometer, ACS Meas. Au. 1 (2021) 35–45. https://doi.org/10.1021/acsmeasuresciau.1c00007.

[83] M. Mamani-Huanca, A.G. de la Fuente, A. Otero, A. Gradillas, J. Godzien, C. Barbas, Á. López-Gonzálvez, Enhancing confidence of metabolite annotation in Capillary Electrophoresis-Mass Spectrometry untargeted metabolomics with relative migration time and in-source fragmentation, J. Chromatogr. A 1635 (2021), 461758. https://doi.org/10.1016/j.chroma.2020.461758.

[84] M. Sugimoto, S. Kikuchi, M. Arita, T. Soga, T. Nishioka, M. Tomita, Large-scale prediction of cationic metabolite identity and migration time in capillary electrophoresis mass spectrometry using artificial neural networks, Anal. Chem. 77 (2005) 78–84. https://doi.org/10.1021/ac048950g.

[85] R. Lee, A.S. Ptolemy, L. Niewczas, P. Britz-McKibbin, Integrative metabolomics for characterizing unknown low-abundance metabolites by capillary electrophoresis-mass spectrometry with computer simulations, Anal. Chem. 79 (2007) 403–415. https://doi.org/10.1021/ac061780i.

[86] M. Sugimoto, A. Hirayama, M. Robert, S. Abe, T. Soga, M. Tomita, Prediction of metabolite identity from accurate mass, migration time prediction and isotopic pattern information in CE-TOFMS data, Electrophoresis 31 (2010) 2311–2318. https://doi.org/10.1002/elps.200900584.

[87] H. Yamamoto, K. Sasaki, Metabolomics-based approach for ranking the candidate structures of unidentified peaks in capillary electrophoresis time-of-flight mass spectrometry: CE and CEC, Electrophoresis 38 (2017) 1053–1059. https://doi.org/10.1002/elps.201600328.

[88] T. Soga, Y. Ohashi, Y. Ueno, H. Naraoka, M. Tomita, T. Nishioka, Quantitative metabolome analysis using capillary electrophoresis mass spectrometry, J. Proteome Res. 2 (2003) 488–494. https://doi.org/10.1021/pr034020m.

[89] A.P. Petrov, L.M. Sherman, J.P. Camden, N.J. Dovichi, Database of free solution mobilities for 276 metabolites, Talanta 209 (2020), 120545. https://doi.org/10.1016/j.talanta.2019.120545.

[90] R. Saito, M. Sugimoto, A. Hirayama, T. Soga, M. Tomita, T. Takebayashi, Quality assessment of untargeted analytical data in a large-scale metabolomic study, JCM 10 (2021) 1826. https://doi.org/10.3390/jcm10091826.

[91] A. Bauermeister, H. Mannochio-Russo, L.V. Costa-Lotufo, A.K. Jarmusch, P.C. Dorrestein, Mass spectrometry-based metabolomics in microbiome investigations, Nat. Rev. Microbiol. 20 (2022) 143–160. https://doi.org/10.1038/s41579-021-00621-9.

[92] P. Phapale, V. Rai, A.K. Mohanty, S. Srivastava, Untargeted metabolomics workshop report: quality control considerations from sample preparation to data analysis, J. Am. Soc. Mass Spectrom. 31 (2020) 2006–2010. https://doi.org/10.1021/jasms.0c00224.

[93] Q. Tian, C.J.G. Duncan, S.J. Schwartz, Atmospheric pressure chemical ionization mass spectrometry and in-source fragmentation of lutein esters, J. Mass Spectrom. 38 (2003) 990–995. https://doi.org/10.1002/jms.514.

[94] J.F. Parcher, M. Wang, A.G. Chittiboyina, I.A. Khan, In-source collision-induced dissociation (IS-CID): applications, issues and structure elucidation with single-stage mass analyzers, Drug Test. Anal. 10 (2018) 28–36. https://doi.org/10.1002/dta.2249.

[95] R.M. Gathungu, P. Larrea, M.J. Sniatynski, V.R. Marur, J.A. Bowden, J.P. Koelmel, P. Starke-Reed, V.S. Hubbard, B.S. Kristal, Optimization of electrospray ionization source parameters for lipidomics to reduce misannotation of in-source fragments as precursor ions, Anal. Chem. 90 (2018) 13523–13532. https://doi.org/10.1021/acs.analchem.8b03436.

[96] P. Purwaha, L.P. Silva, D.H. Hawke, J.N. Weinstein, P.L. Lorenzi, An artifact in LC-MS/MS measurement of glutamine and glutamic acid: in-source cyclization to pyroglutamic acid, Anal. Chem. 86 (2014) 5633–5637. https://doi.org/10.1021/ac501451v.

[97] C. Hu, W. Luo, J. Xu, X. Han, Recognition and avoidance of ion source-generated artifacts in lipidomics analysis, Mass Spectrom. Rev. 41 (2022) 15–31. https://doi.org/10.1002/mas.21659.

[98] Y.-F. Xu, W. Lu, J.D. Rabinowitz, Avoiding misannotation of in-source fragmentation products as cellular metabolites in liquid chromatography–mass spectrometry-based metabolomics, Anal. Chem. 87 (2015) 2273–2281. https://doi.org/10.1021/ac504118y.

[99] J. Xue, R.J.E. Derks, B. Webb, E.M. Billings, A. Aisporna, M. Giera, G. Siuzdak, Single quadrupole multiple fragment ion monitoring quantitative mass spectrometry, Anal. Chem. 93 (2021) 10879–10889. https://doi.org/10.1021/acs.analchem.1c01246.

[100] X. Domingo-Almenara, J.R. Montenegro-Burke, C. Guijas, E.L.-W. Majumder, H.P. Benton, G. Siuzdak, Autonomous METLIN-guided in-source fragment annotation for untargeted metabolomics, Anal. Chem. 91 (2019) 3246–3253. https://doi.org/10.1021/acs.analchem.8b03126.

[101] J. Godzien, E.G. Armitage, S. Angulo, M.P. Martinez-Alcazar, V. Alonso-Herranz, A. Otero, A. Lopez-Gonzalvez, C. Barbas, In-source fragmentation and correlation analysis as tools for metabolite identification exemplified with CE-TOF untargeted metabolomics: CE and CEC, Electrophoresis 36 (2015) 2188–2195. https://doi.org/10.1002/elps.201500016.

[102] M. Skrutková Langmajerová, P. Pelcová, P. Vedrová, A. Celá, Z. Glatz, Capillary electrophoresis–mass spectrometry as a tool for the noninvasive target metabolomic analysis of underivatized amino acids for evaluating embryo viability in assisted reproduction, Electrophoresis 43 (2022) 679–687. https://doi.org/10.1002/elps.202100328.

[103] H. Mori, Y. Morine, K. Mawatari, A. Chiba, S. Yamada, Y. Saito, H. Ishibashi, A. Takahashi, M. Shimada, Bile metabolites and risk of carcinogenesis in patients with pancreaticobiliary maljunction: a pilot study, Anticancer Res. 41 (2021) 327–334. https://doi.org/10.21873/anticanres.14779.

[104] W.H. Wilson Tang, W. Tong, K. Shrestha, Z. Wang, B.S. Levison, B. Delfraino,

B. Hu, R.W. Troughton, A.L. Klein, S.L. Hazen, Differential effects of arginine methylation on diastolic dysfunction and disease progression in patients with chronic systolic heart failure, Eur. Heart J. 29 (2008) 2506–2513. https://doi.org/10.1093/eurheartj/ehn360.

[105] R. Bischoff, H. Schlüter, Amino acids: chemistry, functionality and selected non-enzymatic post-translational modifications, J. Proteonomics 75 (2012) 2275–2296. https://doi.org/10.1016/j.jprot.2012.01.041.

[106] M. Mamani-Huanca, A. Gradillas, A. Gil de la Fuente, Á. López-Gonzálvez, C. Barbas, Unveiling the fragmentation mechanisms of modified amino acids as the key for their targeted identification, Anal. Chem. 92 (2020) 4848–4857. https://doi.org/10.1021/acs.analchem.9b04313.

[107] M. Mamani-Huanca, A. Gradillas, Á. López-Gonzálvez, C. Barbas, Unraveling the cyclization of l -argininosuccinic acid in biological samples: a study via mass spectrometry and NMR spectroscopy, Anal. Chem. 92 (2020) 12891–12899. https://doi.org/10.1021/acs.analchem.0c01420.

[108] T. Kawai, N. Ota, K. Okada, A. Imasato, Y. Owa, M. Morita, M. Tada, Y. Tanaka, Ultrasensitive single cell metabolomics by capillary electrophoresis–mass spectrometry with a thin-walled tapered emitter and large-volume dual sample preconcentration, Anal. Chem. 91 (2019) 10564–10572. https://doi.org/10.1021/acs.analchem.9b01578.

[109] J.T. Aerts, K.R. Louis, S.R. Crandall, G. Govindaiah, C.L. Cox, J.V. Sweedler, Patch clamp electrophysiology and capillary electrophoresis–mass spectrometry metabolomics for single cell characterization, Anal. Chem. 86 (2014) 3203–3208. https://doi.org/10.1021/ac500168d.

[110] P. Nemes, S.S. Rubakhin, J.T. Aerts, J.V. Sweedler, Qualitative and quantitative metabolomic investigation of single neurons by capillary electrophoresis electrospray ionization mass spectrometry, Nat. Protoc. 8 (2013) 783–799. https://doi.org/10.1038/nprot.2013.035.

[111] T. Lapainis, S.S. Rubakhin, J.V. Sweedler, Capillary electrophoresis with electrospray ionization mass spectrometric detection for single-cell metabolomics, Anal. Chem. 81 (2009) 5858–5864. https://doi.org/10.1021/ac900936g.

[112] P. Nemes, A.M. Knolhoff, S.S. Rubakhin, J.V. Sweedler, Metabolic differentiation of neuronal phenotypes by single-cell capillary electrophoresis–electrospray ionization-mass spectrometry, Anal. Chem. 83 (2011) 6810–6817. https://doi.org/10.1021/ac2015855.

[113] J.-X. Liu, J.T. Aerts, S.S. Rubakhin, X.-X. Zhang, J.V. Sweedler, Analysis of endogenous nucleotides by single cell capillary electrophoresis-mass spectrometry, Analyst 139 (2014) 5835–5842. https://doi.org/10.1039/C4AN01133C.

[114] H.-W. Liao, S.S. Rubakhin, M.C. Philip, J.V. Sweedler, Enhanced single-cell metabolomics by capillary electrophoresis electrospray ionization-mass spectrometry with field amplified sample injection, Anal. Chim. Acta 1118

(2020) 36–43. https://doi.org/10.1016/j.aca.2020.04.028.

[115] E.P. Portero, P. Nemes, Dual cationic–anionic profiling of metabolites in a single identified cell in a live Xenopus laevis embryo by microprobe CE-ESI-MS, Analyst 144 (2019) 892–900. https://doi.org/10.1039/C8AN01999A.

[116] R.M. Onjiko, S.E. Morris, S.A. Moody, P. Nemes, Single-cell mass spectrometry with multi-solvent extraction identifies metabolic differences between left and right blastomeres in the 8-cell frog (Xenopus) embryo, Analyst 141 (2016) 3648–3656. https://doi.org/10.1039/C6AN00200E.

[117] R.M. Onjiko, D.O. Plotnick, S.A. Moody, P. Nemes, Metabolic comparison of dorsal versus ventral cells directly in the live 8-cell frog embryo by microprobe single-cell CE-ESI-MS, Anal. Methods 9 (2017) 4964–4970. https://doi.org/10.1039/C7AY00834A.

[118] R.M. Onjiko, E.P. Portero, S.A. Moody, P. Nemes, In situ microprobe single-cell capillary electrophoresis mass spectrometry: metabolic reorganization in single differentiating cells in the live 8-cell frog embryo, Anal. Chem. 89 (2017) 7069–7076. https://doi.org/10.1021/acs.analchem.7b00880.

[119] N. Drouin, A. Mielcarek, C. Wenz, S. Rudaz, Evaluation of ion mobility in capillary electrophoresis coupled to mass spectrometry for the identification in metabolomics, Electrophoresis 42 (2021) 342–349. https://doi.org/10.1002/elps.202000120.

[120] K. Gotoh, Y. Sakaguchi, H. Kato, H. Osaki, Y. Jodai, M. Wakuda, A. Také, S. Hayashi, E. Morita, T. Sugie, Y. Ito, N. Ohmiya, Fecal microbiota transplantation as therapy for recurrent Clostridioides difficile infection is associated with amelioration of delirium and accompanied by changes in fecal microbiota and the metabolome, Anaerobe 73 (2022) 102502. https://doi.org/10.1016/j.anaerobe.2021.102502.

[121] L. Colyn, G. Alvarez-Sola, M.U. Latasa, I. Uriarte, J.M. Herranz, M. Arechederra, G. Vlachogiannis, C. Rae, A. Pineda-Lucena, A. Casadei-Gardini, F. Pedica, L. Aldrighetti, A. López-López, A. López-Gonzálvez, C. Barbas, S. Ciordia, S.M. Van Liempd, J.M. Falcón-Pérez, J. Urman, B. Sangro, S. Vicent, M.J. Iraburu, F. Prosper, L.J. Nelson, J.M. Banales, M.L. Martinez-Chantar, J.J.G. Marin, C. Braconi, C. Trautwein, F.J. Corrales, F.J. Cubero, C. Berasain, M.G. Fernandez-Barrena, M.A. Avila, New molecular mechanisms in cholangiocarcinoma: signals triggering interleukin-6 production in tumor cells and KRAS co-opted epigenetic mediators driving metabolic reprogramming, J. Exp. Clin. Cancer Res. 41 (2022) 183. https://doi.org/10.1186/s13046-022-02386-2.

[122] A. DiBattista, N. McIntosh, M. Lamoureux, O.Y. Al-Dirbashi, P. Chakraborty, P. Britz-McKibbin, Metabolic signatures of cystic fibrosis identified in dried blood spots for newborn screening without carrier identification, J. Proteome Res. (2018). https://doi.org/10.1021/acs.jproteome.8b00351. acs.jproteome.8b00351.